Summer 2020

Modeling the effects of climate change on streamflow and stream temperature in the South Fork of the Stillaguamish River

Katherine Mary Clarke
Western Washington University, clarkekatherinem@gmail.com

Modeling the effects of climate change on streamflow and stream temperature in the South Fork of the Stillaguamish River

Katherine Clarke

Accepted in Partial Completion of the
Requirements for the Degree
Master of Science

ADVISORY COMMITTEE

Dr. Robert Mitchell, Chair

Dr. Douglas Clark

Dr. John Yearsley

GRADUATE SCHOOL

David L. Patrick, Dean

Master's Thesis

In presenting this thesis in partial fulfillment of the requirements for a master's degree at Western Washington University, I grant to Western Washington University the non-exclusive royalty-free right to archive, reproduce, distribute, and display the thesis in any and all forms, including electronic format, via any digital library mechanisms maintained by WWU.

I represent and warrant this is my original work, and does not infringe or violate any rights of others. I warrant that I have obtained written permissions from the owner of any third party copyrighted material included in these files.

I acknowledge that I retain ownership rights to the copyright of this work, including but not limited to the right to use all or part of this work in future works, such as articles or books.

Library users are granted permission for individual, research and non-commercial reproduction of this work for educational purposes only. Any further digital posting of this document requires specific permission from the author.

Any copying or publication of this thesis for commercial purposes, or for financial gain, is not allowed without my written permission.

Katherine Clarke

13 August 2020

Modeling the effects of climate change on streamflow and stream temperature in the South Fork of the Stillaguamish River

A Thesis
Presented to
The Faculty of
Western Washington University

In Partial Fulfillment
Of the Requirements for the Degree
Master of Science

Katherine Clarke
August 2020

Abstract

The Stillaguamish River in northwest Washington State is an important regional water resource for local agriculture, industry, and First Nations tribes and a critical habitat for several threatened and endangered salmonid species, including the Chinook salmon. The river is currently subject to a temperature total maximum daily load, so it is important to understand how projected climate change will affect future stream temperatures and thus salmon populations. Snowpack is the main contributor to spring and summer streamflow and helps to mitigate stream temperatures as air temperatures rise through the summer in the South Fork of the Stillaguamish River. I used gridded historical meteorological data to calibrate the physically-based Distributed Hydrology Soil Vegetation Model and River Basin Model and then applied downscaled, gridded projected climate data to predict how a changing climate will influence hydrology and stream temperature in the South Fork basin through the end of the 21st century.

My projected modeling results predict that increasing air temperatures will cause the South Fork basin to shift from a snow-dominated basin to a rain-dominated basin through the 21st century. This will result in up to a 60% increase in winter streamflow and a 50% decrease in basin-wide snowpack. Snowpack will begin to melt out earlier in the year, resulting in an average 58% decrease in spring and summer streamflow and increased stream temperatures. Average monthly stream temperatures could increase by as much as 6.4 ºC by the 2075 climate normal. The largest increases in stream temperatures occur in the spring due to a reduction in snowmelt. The warmest stream temperatures occur in July due to reduced streamflows and warmer air temperatures. Stream temperatures are projected to increase in every stream segment by the end of the century in the extreme future emissions scenario. Washington State Department of Ecology stream temperature thresholds for salmonid habitat are already being exceeding each year and will be increasingly exceeded through the end of the century. Projected increased stream temperatures will cause additional stress to already endangered salmon species such as Chinook salmon and steelhead trout.

Acknowledgements

This project was funded by the Stillaguamish Tribe of Indians Natural Resources Department, the Geology Department of Western Washington University, the Western Washington University Office of Research and Sponsored Programs, and the Geological Society of America.

I am incredibly grateful to Bob Mitchell, my thesis advisor, for his support, guidance, and patience during the last three years. I could not have completed this project without his support, time, and pressure. I want to thank the employees of the Stillaguamish Tribe of Indians Natural Resources Department for their commitment to the tribe and improving habitat for everyone and everything involved. Their support and commitment have been the driving force behind this project and many other projects intended to improve the quality of life in the Stillaguamish River basin. I would like to especially acknowledge Kip Killebrew for the many days he spent helping me access and establish field sites throughout the South Fork basin. Thank you to John Yearsley for offering his precious retirement time to helping me understand his stream temperature model, the River Basin Model. Thank you to Doug Clark for his feedback throughout this project. I would especially like to thank Kyra Freeman for her guidance every step of the say. Thank you to my professors from Huxley College, Brian Bingham, Robin Matthews, and Jim Helfield. I want to offer a special thank you to Andy Bunn who helped me fix many R scripts. Thank you to Jim Long for helping me learn the ins and outs of running my models on the server. In addition to help from Kyra Freeman, I relied heavily on the previous work of Stephanie Truitt and Ryan Murphy, who paved the way for me. Ryan, Stephanie, and Kyra all wrote R scripts that have greatly accelerated my data analysis process. I would like to thank Maggie for keeping me company and giving me a good reason to take regular writing breaks. Finally, I am so, so grateful for the support of my family and friends over the last three years. I truly could not have made it here without your ongoing and unconditional support.

Table of Contents

Abstract iv
Acknowledgements v
List of Tables vii
List of Figures viii
1.0 Introduction 1
2.0 Methods 8
2.1 Digital Basin Characteristics 9
2.2 Riparian Conditions 9
2.3 DHSVM Hydrology Calibration 10
2.4 Estimation of Mohseni and Leopold Parameters 12
2.5 RBM Stream Temperature Calibration 15
2.6 Projected Simulations 15
3.0 Results 17
3.1 DHSVM Calibration 17
3.2 RBM Calibration 19
3.3 Projected Hydrology 20
3.4 Projected Stream Temperature 20
4.0 Discussion 23
4.1 Model Calibration 23
4.2 Projected Hydrology 25
4.3 Projected Stream Temperature 28
4.4 Comparison to North Fork 31
4.5 Uncertainty and Model Limitations 34
4.6 Future Work 35
5.0 Conclusions 36
6.0 Works Cited 38
7.0 Tables 42
8.0 Figures 54

List of Tables

Table 1. Riparian conditions parameters.....42

Table 2. Statistical tests for analyzing models.....43

Table 3. Global climate models used to project meteorological inputs.....44

Table 4. DHSVM calibration parameters.....45

Table 5. Variable temperature lapse rates for meteorological stations 1 – 4.....46

Table 6. Variable temperature lapse rates for meteorological station 5.....47

Table 7. DHSVM calibration statistical analysis.....48

Table 8. RBM calibration parameters.....49

Table 9. RBM calibration statistical analysis.....50

Table 10. Modeled monthly median streamflow.....51

Table 11. Modeled monthly median stream temperature.....52

Table 12. Modeled average days per year above 16 ºC 7-DADMax.....53

Table 13. Modeled average days per year above 17.5 ºC 1-DMax.....53

Table 14. Modeled average days per year above 22 ºC 7-DADMax.....53

List of Figures

Figure 1. Location of the Stillaguamish River basin.....54

Figure 2. Field sites within the South Fork Stillaguamish River basin.....55

Figure 3. DHSVM calibration to the Ecology gauge.....56

Figure 4. DHSVM low flow calibration to the Ecology gauge.....57

Figure 5. RBM calibration to the Ecology gauge.....58

Figure 6. Modeled median streamflow and SWE at the Ecology gauge and basin average SWE.....59

Figure 7. Modeled average April 1 snowpack extent.....60

Figure 8. Modeled median stream temperature at the Ecology gauge.....61

Figure 9. Verification of CSIRO-Mk3-6-0 as median RCP 8.5 GCM.....62

Figure 10. Modeled mean July stream temperature increase at stream segments.....63

Figure 11. Modeled precipitation and snowmelt.....64

Figure 12. Sub-basins of the South Fork Stillaguamish River basin.....65

Figure 13. Regions of the Stillaguamish River basin with southerly aspects.....66

1.0 Introduction

The Stillaguamish River in northwest Washington State is an important resource for local agriculture, industry, First Nations tribes, and salmonid habitat (Figure 1). The Stillaguamish River provides critical habitat for eight salmonid species, three of which have been classified as threatened by the Endangered Species Act since 1999, including the Chinook salmon (*Oncorhynchus tshawytscha*; SIRC, 2005). The Stillaguamish Tribe depends on the threatened Chinook salmon as the fish are of high cultural and economic importance. Chinook salmon runs occur once in the summer and once in the fall. The summer runs occur May to September, and the fall runs occur September to December (Kip Killebrew, personal communication, 15 March 2018). Projected warming of air temperatures into the 21st century in the Pacific Northwest (PNW) will change hydrology conditions and stream temperatures and further threaten important salmonid habitat and species.

Increasing stream temperatures, due to projected warming climates, are likely to cause stress and migration barriers for anadromous salmon species (Littell et al., 2009). Chinook salmon that use the Stillaguamish River for summer runs are at a particularly high risk. Higher stream temperatures decrease the total dissolved oxygen content, which threatens developing salmon embryos (Wade et al., 2013). High stream temperature is also linked to loss of salmon migration capabilities, which affect how and where salmon will spawn (Wade et al., 2013). The maximum temperature threshold for safe salmonid spawning, rearing, and migration set by the Washington State Department of Ecology (WSDOE) is 16 °C (WSDOE, 2018). The WSDOE has set temperature standards throughout the basin to protect salmonid migration. The 7-day average daily maximum temperature (7-DADMax) is the average of the maximum daily stream temperature for seven consecutive days and is a technique used to measure stream temperatures

that may harm sensitive salmonid species. The maximum allowable 7-DADMax temperature for headwaters is set at 12 °C, middle reaches at 16 °C, and 17.5 °C toward the mouth of the river (WSDOE, 2018). The 16 °C threshold is the maximum temperature for salmon spawning, rearing, and migration. The 17.5 °C threshold is for salmon embryo lethality. For adult salmon, the lethality threshold is 22 °C. Preliminary future climate scenarios modeled for the Stillaguamish River basin by Cao et al. (2016) predict over 50 days a year in which the maximum daily stream temperature at the outlet stream exceeds 20 °C. Days that exceed 20 °C are likely to occur during the warmest summer months, which correspond to the lowest streamflows and unfortunately, the Chinook salmon summer runs.

The Stillaguamish River is currently subject to a total maximum daily load (TMDL; WSDOE, 2015), which means that according to the U.S. Clean Water Act, it does not meet water quality standards in terms of temperature and must be mitigated. Some recommended methods of mitigating stream temperatures include planting riparian buffers along important river reaches, installing engineered log jams to help create deep pools and cold water refugia for aquatic species, including the Chinook salmon, and replanting de-forested areas (SIRC, 2005). Although logging has decreased since the 1990s, it still occurs in the Stillaguamish River basin (SIRC, 2005). One area of note is the totally clear-cut area of about 600 acres surrounding the Jim Creek Naval Radio Station, about 15 kilometers east of Arlington, WA (Boone, 2012).

The Stillaguamish River basin has two major subbasins, the North Fork and the South Fork. My study focuses on predicting changes in streamflow, stream temperature, and snowpack in the South Fork of the Stillaguamish River as a result of projected climate warming through the end of the 21st century. Freeman (2019) conducted a similar study in the North Fork. The South Fork basin drains an area of 660 square kilometers. Surface elevation ranges from about 13 meters at

the confluence of the North Fork and South Fork to just over 2000 meters at the headwaters near Del Campo Peak (Figure 1). Land use in the Stillaguamish River basin is mostly forestry, which is estimated to be around 76%, with the remaining composed of 17% rural, 5% agriculture, and 2% urban (SIRC, 2005).

The historical climate in the Stillaguamish River basin is considered maritime, with warm, dry summers and cool, wet winters. Approximately 20% of the basin is above 1000 meters elevation and is snow-dominated in the winter months. This relatively low elevation range makes the basin particularly sensitive to small changes in winter air temperatures. Small temperature changes influence whether precipitation will fall as snow or as rain at lower elevations; as such the watershed is defined as a rain-snow transitional basin, which is sensitive to climate change (Elsner et al., 2010; Mantua et al., 2010; Vano et al., 2015). The position of the basin in the western foothills of the North Cascades results in a steep orographic precipitation gradient. The 30-year normal precipitation means vary between 1.17 meters at low elevations near the South Fork River mouth to about 4.56 meters near the high elevation peaks (PRISM Climate Group, 2014). Rainfall runoff contributes to streamflow rapidly, whereas snow stores water and contributes to streamflow later while buffering stream temperature as meltwater throughout the spring as air temperatures and day lengths increase (WSDOE, 1981).

Mean annual discharge in the South Fork at WSDOE stream gauge 05A105 (herein called the Ecology gauge; Figure 1) near Granite Falls, WA is approximately 69 cubic meters per second (WSDOE, 2018). The highest discharges occur in the fall and winter, while the lowest occur in the dry season between July and September. Between 2004 and 2009, mean annual stream temperature in the South Fork recorded at the Ecology gauge was 8.8 ºC. The minimum average daily temperature of 0.0 ºC occurred on December 20, 2008, and the maximum average daily

stream temperature of 24.4 ºC occurred on July 29, 2009, which correlates to the warmest air temperature of that period, 41.6 ºC.

A general historical climate warming trend in western Washington has been reported by many studies (e.g., Mote et al., 2014; Mote and Salathé, 2010; Vano et al., 2015). Annual mean temperatures have increased by 0.6 °C to 0.8 °C from 1901 to 2012. In the PNW, global climate models (GCMs) project that the mean air temperature will increase between 3 °C and 7 °C from late 20th century historical mean temperatures through 2099 (Abatzoglou and Brown, 2012; Mote and Salathé, 2010). Previous studies of similar Puget Sound river basins (including the Stillaguamish) predict that the projected increases in average air temperature will change precipitation patterns and result in less overall precipitation in the summer and less precipitation that falls as snow in the winters (e.g., Cao et al., 2016; Dickerson-Lange and Mitchell, 2014; Murphy, 2016; Freeman, 2019). Future trends are expected to increase both the frequency and the intensity of precipitation events in western Washington (Mauger et al., 2016). A 2% to 5% increase per decade of spring precipitation has been observed from 1901 to 2012 (Abatzoglou and Brown, 2012). Climate models used in the Intergovernmental Panel on Climate Change Fifth Assessment Report predict increases in extreme high winter precipitation in western Washington and reductions in snowpack in the Cascade Mountains (Snover et al., 2013). The University of Washington Climate Impacts Group (UW-CIG) predicts that average spring snowpack in Washington will decrease by 38% to 46% by the 2040s and by 56% to 70% by the 2080s. As a result, seasonal streamflow peaks and patterns will change significantly (Snover et al., 2013).

Previous modeling studies in the region have used the Distributed Hydrology Soil Vegetation Model (DHSVM) to predict streamflow and the River Basin Model (RBM) to predict stream temperatures (e.g., Sun et al., 2015; Cao et al., 2016; Truitt, 2018; Freeman, 2019). All of these

studies predicted that earlier snowmelt in the spring and lower streamflow in the summer caused higher stream temperatures.

Cao et al. (2016) used the DHSVM and RBM to study fifteen major rivers, including the Stillaguamish River basin, that discharge to the Puget Sound at a 150-meter gridded resolution. They found that the Stillaguamish River is most at risk and is predicted to have the most days with stream temperatures exceeding 20 °C at the outlet of the river into the Puget Sound. Instream temperatures throughout the Stillaguamish River basin regularly exceed water quality criteria for salmonids and pose a great risk to fish and wildlife that are dependent on cool water sources (WSDOE, 2015). In general, adult Chinook salmon will not migrate upstream if temperatures are above 20 °C (Bergendorf, 2002). The lethal threshold for adult Chinook salmon is a 7-DADMax of 22 °C or a 1-day average maximum temperature of 23 °C (WSDOE, 2002).

The South Fork of the Nooksack River is about 70 kilometers north of the confluence of the North and South forks of the Stillaguamish River basin and has similar topography, elevation, and a lack of glaciers. Murphy (2016) used the DHSVM and projected climate data to model streamflow in the South Fork of the Nooksack River basin and predicted over a 75% median reduction in basin-average snow-water equivalent (SWE) and a doubling of winter streamflows due to the reduced snowpack and projected warmer, drier summers. Truitt (2018) used the hydrology outputs from Murphy (2016) and the RBM to model projected stream temperature in the South Fork of the Nooksack and predicted late summer mean daily stream temperatures to increase by as much as 40% with many days exceeding 20 °C.

Freeman (2019) employed the DHSVM and RBM to examine the effects of projected climate change on the North Fork of the Stillaguamish River (Figure 1). Results are comparable to the physically similar South Fork Nooksack River (Truitt, 2018). Winter precipitation is expected to

change from mixed rain-and-snow-dominated to rain-dominated throughout the 21st century, leading to increased winter runoff, higher streamflows, and a decrease in SWE, resulting in lower spring and summer streamflows. Stream temperatures are expected to increase into the 21st century as a result of increasing air temperatures and changes in streamflow trends. Freeman (2019) found that decreases in snowpack and snowmelt runoff will cause the greatest stream temperature increases in late spring. These effects are expected to become increasingly pronounced later in the century, particularly under the extreme emissions scenario RCP 8.5.

I calibrated the DHSVM and RBM to the South Fork of the Stillaguamish River basin to historical gridded data and used the calibrated models with projected climate data to predict changes in streamflow and stream temperature through the 21st century. The models are physically based and spatially distributed and have been applied to the Stillaguamish River basin and similar mountainous terrains in the PNW (Cao et al., 2016; Murphy, 2016; Truitt, 2018; Freeman, 2019). To improve upon the work of Cao et al. (2016), I use a finer spatial resolution of 50 meters to account for smaller scale variation in topography and vegetation. I also use more detailed riparian characteristics, including more specific vegetation type along individual reaches and specific widths of stream segments along the entire mainstem of the South Fork.

I compared the projected results from the South Fork to those of Freeman (2019), who completed a similar study in the North Fork basin of the Stillaguamish River. The North Fork basin and the South Fork basin are similar in relief and size; however, the mainstem valley of the North Fork is much wider than the mainstem valley of the South Fork. The North Fork once drained the upper Skagit River, the Sauk River, and the Suiattle River until the retreat of the Cordilleran ice sheet and a plug of Vashon-aged sediment blocked the Skagit River valley and diverted these rivers away from the North Fork Stillaguamish drainage (Booth et al., 2003). The

wider, sediment-filled valley of the North Fork may allow a larger groundwater influence in the river during the warmer summer months that may cool the stream water. The South Fork basin also has a dominantly east-west trend, which may influence the degree of solar radiation inputs to streams. Although the North Fork has a general east-west trend, it has large tributary sections with a southerly aspect. This difference in aspects basins influences the degree of solar radiation and warming of streams throughout the year.

2.0 Methods

I applied the DHSVM and RBM to examine changes in streamflow and stream temperature trends in the South Fork of the Stillaguamish River basin into the 21st century to identify general trends and reaches of the South Fork basin that are particularly at risk for changing streamflows and increasing stream temperatures. I accomplished this by the following scope of work:

1. Used ArcGIS software to create 50-meter gridded digital basin spatial characteristics using publicly available data from government agencies.
2. Assessed riparian buffer characteristics along stream segments using ArcGIS software and first and last return lidar data.
3. Calibrated the DHSVM using gridded historical meteorological data and historical Ecology gauge streamflow data and regional snow data.
4. Conducted field work to collect data for estimating streamflow parameters for the RBM
5. Calibrated the RBM using gridded historical meteorological data and historical temperature data from Ecology and the Stillaguamish Tribe.
6. Performed simulations of the DHSVM and the RBM using downscaled projected meteorological data to estimate projected streamflow and stream temperatures.
7. Statistically analyzed results and identified reaches that are most at risk for temperature increases and streamflow changes.
8. Compared simulation results of the South Fork to results of the North Fork.

2.1 Digital Basin Characteristics

The DHSVM and the RBM are spatially distributed models and require gridded digital basin characteristics. Detailed procedures for processing the digital inputs using ArcGIS are outlined in previous MS theses (e.g., Murphy, 2016; Freeman, 2019). Lidar data, available from the Washington State Department of Natural Resources, were resampled to a 50-meter resolution for the South Fork basin. Land cover data (2011), available at 30-meter resolution from the National Oceanic and Atmospheric Association (NOAA), were resampled to a 50-meter resolution and converted to DHSVM classifications. Soil type data were acquired from the United States Department of Agriculture STATSGO soil database. The soil thickness layer and stream network were created using a Python-ArcGIS script developed for the DHSVM. The soil thickness ranges from one to five meters, and there are 906 individual stream segments in the South Fork basin.

2.2 Riparian Conditions

Riparian conditions along each stream segment are required for the DHSVM to produce energy outputs that are necessary as inputs for the RBM (Table 1). Parameters for riparian conditions include buffer width, vegetation height within the buffer zone, extinction coefficient, canopy-bank distance, stream width, and overhang coefficient. The buffer zone width of 10 meters, canopy-bank distance of 0 meters, and overhang coefficient of 0.01 were the values used by Cao et al. (2016) for each stream segment. To estimate variable vegetation height and type in the riparian zone, I used first and last return lidar data to determine average vegetation height in the 10-meter buffer zone along each of the 906 stream segments in the basin following the procedures outlined in Freeman (2019). The average leaf area index (LAI) was estimated based on the dominant DHSVM land cover vegetation type in the 10-meter buffer zone along each stream segment. The LAI is used to express how much light is able to penetrate the canopy. The

extinction coefficient (*k*) was estimated using LAI and the following relationship from Sun et al. (2015):

$$k = \frac{LAI}{64} \quad (1)$$

Stream width was estimated at each stream segment along the mainstem of the South Fork from Google Earth Pro and ranged from 10 to 70 meters, with tributary widths set constant at 10 meters.

2.3 DHSVM Hydrology Calibration

The DHSVM was developed at the University of Washington and the Pacific Northwest National Lab (PNNL; Wigmosta et al., 1994) and has been applied extensively to mountainous watersheds throughout the PNW (e.g., Cao et al., 2016; Dickerson-Lange and Mitchell, 2014; Cuo et al., 2008; Sun et al., 2015; Murphy, 2016; Truitt, 2018). DHSVM version 3.1.2 was modified to output energy and streamflow information that is required for the RBM by Ning Sun at the PNNL. The DHSVM uses gridded, spatial inputs to define the basin including a digital elevation model, soil type, vegetation type, soil depth, and a stream network. Given meteorological inputs (forcings), the DHSVM uses physical and empirical relations with spatial characteristics to calculate an energy and water budget throughout the basin. The DHSVM simulates several hydrology variables, including evapotranspiration, snow accumulation and melt, soil storage, and streamflow. The smaller 50-meter resolution allows the model to read more detailed variability in topography, soil type, soil depth, and vegetation, and to distribute meteorological inputs, which then produces a more accurate representation of the energy and hydrology of the river basin.

To calibrate the DHSVM, I used gridded, historical, meteorological data developed by Livneh et al. (2013). The gridded data are at 1/16th degree latitude and longitude and contain

daily time series of climate variables at gridded points (Livneh nodes) from 1950 to 2013. The publicly available daily Livneh data were bias-corrected and disaggregated into three-hour time steps by the University of Washington Climate Impacts Group (Mauger et al., 2016). Meteorological variables required for the DHSVM include air temperature (°C), wind speed (m/s), percent humidity, solar radiation (W/m^2), longwave radiation (W/m^2), and precipitation (m).

Calibration of the DHSVM was achieved based on comparison to historical observed streamflow at Ecology gauge 05A105 at the Jordan Road Bridge in Granite Falls, WA (Figure 1). I used a five-year calibration period of 2004 to 2009 based on the availability of continuous streamflow and stream temperature data. Only five whole water years of continuous stream temperature data were available, and I wanted to keep the calibration periods consistent.

I used four statistical tests to assess model skill (Table 2) based on the work of Moriasi et al. (2007). The performance evaluation criteria (PEC) for these tests were meant to evaluate model skill for discharge (DHSVM). Although these criteria were not specifically designed for evaluating stream temperature models, I used the same tests as a benchmark for RBM skill, similar to the criteria of Freeman (2019). The main statistical test that I used was the Nash-Sutcliffe efficiency (NSE) coefficient (Nash and Sutcliffe, 1970), which compares daily mean observed streamflow or temperature to daily mean simulated or predicted streamflow or temperature. An NSE value greater than 0.5 indicates a satisfactory model skill (Moriasi et al., 2007, 2015). The NSE is a more rigorous test than the standard R^2 statistical test. Pearson's coefficient of determination, R^2, describes the portion of total variance in the observed data (O) that is explained by the model simulated data (P). An R^2 value greater than 0.60 indicates

satisfactory model skill (Moriasi et al., 2007, 2015). Information on other statistical tests used for assessing model skill (RSR and PBIAS) can be found in Table 2.

I focused on optimizing model skill during the months of lowest flow and highest temperature, May to September, because I am concerned with future streamflows and stream temperature for salmonid habitat and migration. I also examined the snow water equivalent maps output by the DHSVM to ensure a reasonable amount and extent of snow basin-wide. Following methods of Freeman (2019), I output the SWE at each grid cell in the South Fork basin on April 1 for each year of the calibration period and produced maps in ArcGIS. There is not a SNOTEL (SNOwpack TELemetry) station in the Stillaguamish basin so I used the nearby Skookum Creek SNOTEL station as a proxy to compare model outputs. The Skookum Creek SNOTEL station is at an elevation of 1009 meters and about 50 kilometers southeast of the South Fork basin. Using ArcGIS, I extracted a 100-meter band from the simulated output at 1000 meters and compared the mean SWE of the band to observed historical snowpack at the Skookum Creek SNOTEL station.

2.4 Estimation of Mohseni and Leopold Parameters

The RBM is a semi-Lagrangian, one-dimensional stream temperature model that is scalable in space and time (Yearsley, 2009, 2012; Sun et al., 2015). The model requires initial headwater temperatures, tracks parcels of water through the river basin, and estimates stream segment temperatures as influenced by net solar radiation, net longwave radiation, sensible heat flux, latent heat flux, groundwater, and advected heat from adjacent tributary segments. Other than riparian characteristics along stream segments, there are eleven variables required for the calibration and operation of the RBM, including those in the Mohseni relation used to estimate the initial headwater temperatures, and the Leopold parameters used to estimate the stream

velocity and depth from the DHSVM discharge values. Two other calibration parameters include the minimum stream depth and the minimum stream velocity. To estimate magnitudes for these, I conducted field work at eleven sites (Figure 2) throughout the South Fork basin during the summer and fall of 2018. I visited each site at least twice to collect data on streamflow, stream temperature, and stream morphology at low and high magnitudes of discharge.

Estimation of Mohseni parameters requires observed stream temperatures and observed air temperatures. Observed stream temperatures were collected from the field, and estimated air temperatures were taken from publicly available gridded climate data (PRISM Climate Group, 2014). Initial headwater conditions (T_{head}, °C) in the RBM are estimated based on relating headwater temperature to air temperature in the following equation:

$$T_{head} = \mu + \frac{\alpha - \mu}{1 + e^{\gamma(\beta - T_{smooth})}} \quad (2)$$

where α is an estimate of the maximum headwater temperature (°C), β is the air temperature at the inflection point of the function (°C), γ is the steepest slope of the function (ratio), and μ is the minimum headwater temperature (°C; Mohseni et al., 1998). The smoothing parameter (T_{smooth}, unitless) is used to manage high frequency fluctuations in air temperature (T_{air}, °C) in the following equation:

$$T_{smooth} = \tau * T_{air}(t) + (1 - \tau) * T_{air}(t - 1) \quad (3)$$

where t is the time step and

$$\tau = \frac{1}{(smoothing\ period)} = \frac{1}{(7\ days * 8\ timesteps\ per\ day)} \quad (4)$$

In 2018, employees of the Stillaguamish Tribe of Indians Natural Resources Department installed HOBO TidbiT v2 Water Temperature Data Loggers in the river at the same eleven sites

where streamflow data were collected throughout the South Fork basin to record stream temperature every 30 minutes (Figure 2). The data loggers were installed using the method developed by Killebrew et al. (2018). The water temperature data loggers have an accuracy of ± 0.2 °C up to 50 °C and a resolution of 0.02 °C up to 25 °C. Temperature data sets ranged from 5 months to 18 months. Of these eleven sites, ten were used to estimate Mohseni parameters. One temperature logger was lost either to strong currents and rocks or tampering. Stream temperature data from the Ecology gauge at Granite Falls (Figure 1) were also used in Mohseni calculations.

Leopold parameters are required for the RBM to estimate stream depth and velocity from discharge data produced by the DHSVM. Estimation of the Leopold parameters requires observed stream morphology, velocity, and depth relationships.

$$D = aQ^b \tag{5}$$

$$u = cQ^d \tag{6}$$

Where Q is discharge (cms), D is depth (m), u is velocity (m/s), and a, b, c, and d are empirical constants.

Field measurements, including stream discharge, depth, and width, were made at eleven sites throughout the South Fork basin in order to estimate the empirical constants. I also estimated stream widths of the mainstem using an orthophoto and a measuring tool in Google Earth Pro. I considered stream width to be the distance from bank to bank at the vegetation line. These sites correlated to the sites with continuous stream temperatures loggers (Figure 2). Stream discharge was measured twice in the summer and fall of 2018 following the USGS stream gauging measurement technique (Turnipseed and Sauer, 2010). Stream discharge was estimated by measuring channel width and depth with a wading rod and surveying measuring tape. Stream velocity was recorded across a transect of the stream with a Marsh-McBirney Flo-Mate 2000

Portable Flow Meter. Streamflow data from the Ecology gauge at Granite Falls were also used in estimating the Leopold parameters. Mohseni and Leopold parameters were adjusted to optimize the skill of the calibrated model. Calibration of the model requires manipulation of eleven variables. I systematically adjusted each variable and examined its influence on simulated stream temperature and its effect on the statistics of overall model skill based on a range of values for each parameter. I was informed on the range of values for each parameter by John Yearsley and Kyra Freeman based on her previous work with the RBM.

2.5 RBM Stream Temperature Calibration

The RBM was calibrated to a five-year period from water years 2004 to 2009 based on availability of continuous recorded stream temperature data from the Ecology gauge. I used the Nash-Sutcliffe efficiency coefficient again to assess model skill and the same statistical tests recommended by Moriasi et al. (2007, 2015; Table 2). Moriasi et al. (2007, 2015) do not specifically address criteria for stream temperature modeling, but I used the same statistical tests and performance evaluation criteria as the DHSVM streamflow as a benchmark for determining the RBM skill.

In accordance with Washington State water quality standards, I also calculated the number of observed days exceeding the 16 °C 7-DADMax and tried to match the number of simulated days exceeding the 16 °C 7-DADMax to the observed value. In order to optimize model skill for the warmest months of the year, I also performed the same four statistical tests from Table 2 on the model calibration for the months of May to September in addition to annual data.

2.6 Projected Simulations

I used the calibrated DHSVM and RBM to simulate streamflow and stream temperatures in the South Fork basin of the Stillaguamish River for water years 2009-2099. I forced the DHSVM

with projected climate data from ten different GCMs and applied two different emissions scenarios – representative concentration pathways (RCPs) 4.5 and 8.5 (Table 3). The GCMs were developed by various organizations as part of the Climate Model Intercomparison Project Phase 5 (CMIP5) and downscaled to a regional scale (Abatzoglou and Brown, 2012). I used the ten GCMs determined by Rupp et al. (2013) to be the most suitable for the PNW (Table 3), the same forcings used by Freeman (2019) in the North Fork. RCP 4.5 is a median warming scenario associated with moderate anthropogenic changes, which produces approximately 2 °C global warming. RCP 8.5 is an extreme warming scenario associated with few to no anthropogenic changes, continued high emissions, and produces approximately 4-5 °C global warming. The climate scenarios were downscaled to the basin using the multivariate adaptive constructed analogs (MACA) method (Abatzoglou and Brown, 2012). The daily time series was bias-corrected and disaggregated into DHSVM inputs at three-hour time steps by the UW-CIG (Mauger et al., 2016).

To predict future trends in streamflow and stream temperature, I analyzed the projected models' simulation results in 30-year intervals centered on the years 1996 (hindcast), 2025, 2050, and 2075 because climate trends usually occur in 30-year climate normals. For example, I analyzed the medians for the years 2010 to 2040 to represent the 2025 30-year climate normal.

3.0 Results

3.1 DHSVM Calibration

There are 33 Livneh nodes within and surrounding the South Fork basin that contain historical meteorological data in daily values. These data sets were disaggregated into three-hour time steps and bias-corrected by the UW-CIG to account for variability in topography and orographic effects and are used as gridded meteorological inputs to the DHSVM. Because the data were disaggregated from daily values to three-hour time steps, intense precipitation events are not necessarily accurately represented. Short and strong precipitation events are dispersed over eight three-hour periods throughout one day and may not appear to be as strong once disaggregated. Because of this, peak winter flows are not fully captured. The Livneh nodes are set on a $1/16^{th}$-degree grid and may not accurately represent drastic changes in small areas of relief in the higher elevation parts of the basin. I grouped the 33 Livneh nodes by both elevation and spatial location and plotted precipitation and air temperature time series for each of the nodes to identify biased stations. From these groups, I omitted nodes that showed excessive differences based on elevation or spatial location. I ran simulations of the DHSVM using the remaining nodes until the model produced reasonable streamflow outputs. I isolated five Livneh node locations to use in further refining the DHSVM (Figure 2).

The DHSVM is sensitive to temperature and precipitation lapse rates, rain and snow temperature thresholds, lateral and horizontal soil conductivities, and select other soil characteristics (Table 4). Temperature and precipitation lapse rates can be set as constant values or variable values by month (Tables 5-6). I adjusted these model parameters until I achieved an acceptable model skill for simulated streamflow and a reasonable basin-wide SWE. Freeman

(2019) found that April is most influential for snowmelt and October is most influential for initial snow accumulation.

DHSVM streamflow calibration was achieved at the Ecology gauge for water years 2004-2009 with an overall daily mean flow NSE of 0.464 and a monthly mean flow NSE of 0.854, which meet the PEC standards of Unsatisfactory and Good, respectively (Figure 3; Table 7; Moriasi et al., 2015a). The overall R^2 value was 0.477 and the monthly R^2 value was 0.895, which meet the guidelines of Moriasi et al. (2015a) of Unsatisfactory and Good, respectively. The lower results for annual daily statistical tests are a result of winter peak flows not being fully captured in part due to the way the meteorological data were disaggregated. I focused on improving statistics for the calibration for the lowest flow months of May to September when stream temperatures are highest and salmonid species are most at risk. The low flow daily NSE value was 0.618 and R^2 value was 0.686, which meet the PEC of Good and Good, respectively (Figure 4; Table 7).

Achieving an acceptable calibration for streamflow was dependent on simulating a representative SWE in the basin. Trends in snowpack from year to year at the Skookum Creek SNOTEL station are similar to trends in basin-wide SWE modeled by the DHSVM in the South Fork basin. The average April 1 SWE at the Skookum Creek SNOTEL station (~1000 meters elevation) over the calibration period was about twice as much as the modeled average April 1 SWE in the South Fork basin, meaning overall modeled snow accumulation was at higher elevations. Although I may be underestimating SWE at 1000 meters, I believe my overall basin-wide SWE is reasonable because I am achieving good spring and summer streamflow calibration due to snowmelt (Figure 4).

3.2 RBM Calibration

Mohseni parameters for the RBM were estimated from continuous water logger temperature data (Figure 2) and PRISM Climate Group (2014) air temperature data. The PRISM data are taken from the PRISM standard 4-kilometer grid resolution. The topography and air temperature in the South Fork basin can be highly variable, and comparing one field site along the stream to a 4-kilometer grid cell offers an estimate of parameters required for the RBM rather than an exact value. When snowmelt is highest during the spring and early summer, the Mohseni method overestimated stream headwater temperatures. To correct this, I invoked a snowmelt algorithm in the RBM similar to that applied by Freeman (2019) and Truitt (2018). The snowmelt algorithm fixes headwater temperatures to 7 °C when the basin-wide average snowmelt volume from the DHSVM reaches a predefined threshold of 0.0002 m^3/3 hours. When the basin average snowmelt is below the threshold, the model invokes the Mohseni relation to estimate the initial headwater temperatures.

I started RBM calibration by adjusting the average values for the Mohseni parameters estimated from all field sites. My parameter adjustments were in part informed by the sensitivity analyses and RBM modeling performed by Freeman (2019). Values that produced the best model skill with realistic temperature outputs are listed in Table 8. The RBM annual calibration was achieved at the Ecology gauge for water years 2004-2009 with an overall daily mean NSE value of 0.927 and an R^2 value of 0.928, meeting the PEC of Very Good and Very Good, respectively (Figure 5; Table 9). Calibration was achieved for low flow and high temperature months (May to September) with a daily NSE value of 0.856 and an R^2 value of 0.875, meeting PEC standards of Very Good and Good, respectively (Table 9). I also assessed the fit of high stream temperatures by comparing the average number of days per year observed above the 7-DADMax threshold

temperature of 16 °C to the simulated average number of days above the same threshold. The observed average was 181 days (9.9%) and the simulated average was 242 days (13.3%).

3.3 Projected Hydrology

The daily median historical (30-year hindcast) simulated hydrograph exhibits the highest streamflow in November with a distinct dip in December (Figure 6). As snow melts through the spring (i.e., freshet), streamflow reaches another peak in May, slightly lower than the November peak. After May, streamflow decreases through the summer with the lowest flow in September. Projected monthly median streamflows increase from November through March through the 21st century in both the RCP 4.5 and RCP 8.5 scenarios (Table 10). Overall, streamflow gradually decreases in late winter. After April, streamflow decreases significantly through late summer (Figure 6; Table 10).

Average basin-wide historical SWE peaks at ~0.3 meters in late March and early April and decreases to 0 meters by July (Figure 6). Future projected SWE decreases significantly through the end of the 21st century with the lowest scenario being RCP 8.5 in 2075. Late in the century, the SWE peaks in February and melts out entirely by May (Figure 6). Snow maps output by the DHSVM and averaged over each 30-year climate normal show the extent of snowpack receding to higher elevations in the South Fork basin by 2075 (Figure 7).

3.4 Projected Stream Temperature

At the Ecology gauge, historical (30-year hindcast) simulated stream temperature peaks in August with a monthly median of approximately 15.3 °C and minimums of approximately 3 °C in December and January (Table 11; Figure 8). For the 2025 climate normal, there is a slight increase in monthly median temperatures when compared to the hindcast results. July has the greatest increase in temperature of 2.7-2.9 °C. The maximum median temperature reaches 16 °C

in July and August, which is the threshold for core salmon migration, rearing, and spawning. There is a difference of 0.1 to 0.2 °C between the RCP 4.5 and RCP 8.5 scenarios in July and August in the 2025 climate normal (Figure 8; Table 11). Note that the plots in Figure 8 represent daily medians, so there are likely times during the day when the stream temperatures exceed the daily and monthly (Table 11) medians.

For the 2050 climate normal, the greatest increase in monthly median stream temperature at the Ecology gauge is 4.5 °C in June and 3.1 °C July, with the peak temperature shifting to 16.8 °C and 17.2 °C in July for RCP 4.5 and RCP 8.5, respectively. Median temperatures for RCP 4.5 in July and August are projected to be 16.8 °C and 16.3 °C, respectively, which exceed the migration and spawning temperature threshold. Median temperatures for RCP 8.5 in July and August are projected to be 17.2 °C and 16.5 °C, respectively, which both exceed the salmon migration and spawning threshold. In the 2050 climate normal, all projected RCP 8.5 temperatures are higher than the projected RCP 4.5 temperatures (Figure 8; Table 11).

By the 2075 climate normal, the highest monthly median temperature is 18.1 °C in July in the RCP 8.5 scenario (Table 11). The projected peak stream temperature has shifted from August in the hindcast to July in the 2075 climate normal. August is projected to be approximately 0.7 to 1.0 °C cooler than July in 2075 and 1.3 to 1.8 °C warmer than the hindcast August temperatures (Figure 8; Table 11).

The hindcast stream temperature simulation averages 40 days per year that exceed the 16.0 °C 7-DADMax threshold for core salmon migration and spawning at the Ecology gauge. During the 2075 climate normal, the RCP 4.5 scenario projects an average of 85 days per year exceeding that threshold, a 215% increase, and the RCP 8.5 scenario projects an average of 110 days per year exceeding that threshold, a 275% increase (Table 12).

July is expected to have the warmest stream temperatures by the 2075 climate normal and sees increases in stream temperatures in every stream segment when modeling the CSIRO-Mk3-6-0 GCM under RCP 8.5 conditions and the hindcast temperatures. The CSIRO-Mk3-6-0 GCM is approximately the median climate model of all ten GCMs (Figure 9). Temperature increases in individual segments vary from a minimum of 3.1 °C to a maximum of 8.3 °C, with an average stream segment temperature increase of 6.5 °C (Figure 10).

4.0 Discussion

4.1 Model Calibration

The hydrology of the South Fork proved difficult to calibrate mainly due to the rapid changes in topography, some unreliable meteorological grid cells, and trying to find a balance between streamflow and snowpack. The historical Livneh forcing data are a daily time series of maximum and minimum temperature, precipitation, and wind speed (Livneh et al., 2013). The daily time series were disaggregated to a three-hour time series of temperature, wind speed, humidity, shortwave radiation, longwave radiation, and precipitation. When the daily data were disaggregated to three-hour time steps, short and strong storm events were spread across a 24-hour period, dampening the intensity of winter storms and their influence on streamflow. Because of this, annual NSE values are a bit less than 0.5, the acceptable value for hydrologic models. Cao et al. (2016) achieved a higher NSE score than I did for annual streamflow. Cao et al (2016) calibrated the DHSVM for the Stillaguamish to USGS gauge 12167000 in the North Fork of the basin, while I worked specifically in the South Fork. Freeman (2019) also achieved NSE values greater than 0.5 in the North Fork. I tried to find a realistic balance between snow accumulation throughout the South Fork basin and snowmelt contributing to streamflow in the spring and early summer. Since summer streamflow and stream temperatures are the focus of my study, I concentrated on achieving an acceptable calibration for low flow months (May-September). The DHSVM accounts for groundwater input to the stream, but it can be difficult to accurately quantify groundwater flow. I achieved calibration of the model in part by adjusting soil conductivities, increasing the maximum soil depth to 5 meters, and adjusting temperature and precipitation lapse rates to increase the modeled winter snowpack. By adjusting soil conductivities and storage parameters (e.g., porosity and field capacity), I was able to control the groundwater input to streams and achieve a realistic level of spring and summer streamflows.

Winter flow trends, particularly peak flows, are not accurately simulated in this project, but may be able to be improved in the future with improved forcing data, such as a new meteorological data set informed by the Weather Research and Forecasting (WRF) model (Mauger et al., 2018).

To achieve reasonable modeled spring and summer flows, I adjusted temperature and precipitation lapse rates to control the amount of snow accumulation, which resulted in less snowpack than expected at elevations near 1000 meters, when compared to the Skookum Creek SNOTEL site. The modeled SWE in the South Fork basin only accounted for about 50% of the average SWE at the Skookum Creek SNOTEL station; however, the modeled SWE output trends do follow similar trends to historical observed SWE at Skookum Creek. There are no SNOTEL stations in the Stillaguamish River basin to compare simulated snow outputs to, so I used SWE from the Snohomish River basin Skookum Creek SNOTEL station, which is approximately 70 kilometers southeast of Arlington. Freeman (2019) used the Skookum Creek SNOTEL station as a benchmark for comparing snow output because of its similar elevation to the Stillaguamish basin and its location on the west side of the Cascades. Her modeled historical SWE magnitudes in the North Fork more closely matched magnitudes at the Skookum Creek SNOTEL. It is important to note that calibrating a basin-wide value to a single point is not the most reliable method but is the best method possible within the scope of this study. As stated above, although I may be underestimating SWE at 1000 meters, I believe the overall basin-wide SWE is reasonable because I am achieving good spring and summer streamflow calibration due to snowmelt (Figure 4).

The tests used for RBM calibration analysis are based on statistical tests meant for discharge, not temperature. I used the same tests as guidelines for temperature model skill, keeping the same requirements for both the DHSVM and RBM model skills. RBM calibration proved

difficult due to odd summer discharges in 2005 and 2006, which may be a result of spring streamflows not being fully captured by the DHSVM.

Calibration of the RBM could be improved by refining estimation methods of the Leopold and Mohseni parameters. For this project, I used air temperature from PRISM climate data at a 4-kilometer scale along with water temperature recorded by TidbiT data loggers at specific sites along stream segments throughout the basin. This method could be improved by installing air temperature loggers at the same sites as the water temperatures loggers to better estimate the relationship between air and water temperatures at each field site and temperature lapse rates in regions of the basin toward higher elevations.

4.2 Projected Hydrology

The historical streamflow hindcast at the Ecology gauge shows streamflow peaking in November when precipitation increases and declining into the winter as precipitation changes to snow and higher elevation snowpack begins to develop (Figure 6). Snowpack starts developing in November and reaches a peak in April. In the spring, snowpack melts and the runoff contributes to streamflow, increasing streamflow to a secondary peak at the end of May (i.e., freshet). Streamflow then decreases through the summer as snowpack melts out and precipitation decreases (Figure 6).

In general, simulated projected streamflow into the 21st century at the Ecology gauge in the in the South Fork of the Stillaguamish River increases in the late fall and winter and decreases in spring and summer, consistent with other western Cascade modeling studies (e.g., Murphy, 2016; Freeman, 2019; Vano et al., 2010; Cuo et al., 2008; Cao et al, 2016; Lee et al., 2020; Mauger et al., 2016). These changes are a direct result of the projected reduction in snowpack.

Increasing air temperatures into the 21st century transition the basin from a mixed rain-and-snow basin to a rain-dominated basin, resulting in a basin average SWE that decreases steadily throughout the century, similarly to that of the North Fork of the Stillaguamish River (Freeman, 2019), the South Fork of the Nooksack River (Truitt, 2018), and other modeling studies of western Washington watersheds (e.g., Tohver and Hamlet, 2010; Lee et al., 2020; Mauger et al., 2016; Morgan et al., 2017). Snowpack forms later in the year and melts out earlier, which reduces spring and summer streamflow. Historically, peak SWE occurs around mid-April but shifts earlier to February by 2075 (Figure 6). As early winter precipitation changes to mostly rain, winter streamflows increase. By 2075, peak streamflows shift to late November and early December. As discussed in Freeman (2019), there is a notable dip in streamflow in December due to a low-precipitation bias in December, which also affects the downscaled MACA data (Figure 11; Abatzoglou and Brown, 2012). The December precipitation bias does not have a significant effect on summer streamflow and temperatures.

Figure 11 shows increased snowmelt from February to April in the hindcast and the 2025 climate normal as a result of rain-on-snow events. Historically, snowmelt continues to occur and contribute to streamflow through the early summer and into the beginning of August. This snowmelt helps to mitigate stream temperatures as air temperatures rise in the summer. However, as air temperature increases and snowpack decreases into the 21st century, rain-on-snow events are less frequent and less pronounced in magnitude in snowmelt plots. By the 2075 climate normal, peak snowmelt occurs in January and decreases until June when there is almost no snowmelt contributing to and mitigating streamflow (Figure 11). By the 2075 climate normal in the extreme emissions scenario, there is essentially no snowpack contributing to summer

streamflow, and summer flow becomes very low. The RCP 8.5 emissions scenario shows the most extreme effects of climate change on the South Fork basin by 2075.

As found in previous modeling studies (Freeman, 2019; Murphy, 2016), there is not a significant difference in modeled streamflows and SWE between the moderate (RCP 4.5) and severe (RCP 8.5) emissions until after the mid-21st century (Figure 6). By 2075, the differences in streamflow and SWE trends are more easily identifiable between the RCP 4.5 and RCP 8.5 scenarios. The RCP 4.5 scenario includes greenhouse gas emissions that would be decreased immediately, but the large-scale effects of that may not be seen for several decades after curbing emissions. The climate response to a projected forcing may lag as little as one decade or as much as a century, depending on the sensitivity of the climate (Hansen et al., 2005).

Transient river basins, like the Stillaguamish, are predicted to have dramatically increased winter flood magnitudes and frequencies in the future as they evolve into rain-dominant basins (Mantua et al., 2010). The DHSVM underpredicts peak winter streamflows (Figure 3), in part due to the attenuation of high intensity storm events due to the disaggregation of the Livneh meteorological data into three-hour time steps. High intensity precipitation events contribute runoff to streams faster and cause higher peaks in discharge. Future work on evaluating winter flood risks would require an improved meteorological data set. James Robinson, an M.S. graduate student at Western Washington University, is currently applying new WRF-derived meteorological data at one-hour time steps to analyze peak streamflows in the entire Stillaguamish River basin.

4.3 Projected Stream Temperature

Simulated projected stream temperatures increase into the 21st century at the Ecology gauge in the South Fork Stillaguamish River during all months of the year by the 2075 climate normal (Table 11; Figure 8). These changes are a result of increased air temperatures, decreased snowpack, and a reduction in summer streamflow.

The most dramatic change in stream temperatures occurs in June in both emissions scenarios. There is an increase of 4.9 °C from historical to 2075 temperatures under RCP 4.5 and an increase of 6.4 °C from historical under RCP 8.5 by the end of the century (Table 11). The large increase is primarily the result of the reduced snowpack and a lower snowmelt contribution to spring and early summer streamflow in the 21st century. Normally the RBM predicts the initial headwater temperatures using air temperatures and the Mohseni relation (Equation 2). The version of the RBM that I used has a snowmelt algorithm that decreases the initial headwater temperatures to compensate for the input of cool water delivered by snowmelt in the higher elevation portions of the basin. The RBM algorithm applies fixed cool headwater temperatures when a snowmelt threshold (produced by the DHSVM) is reached. The RBM algorithm reverts to the air temperature-based Mohseni relation to estimate headwater temperatures when the basin average snowmelt is below the snowmelt threshold. As snowpack and snowmelt decrease into the 21st century, the snowmelt threshold is typically below the predefined threshold, meaning that the headwater temperatures are invoked by the Mohseni relation and the warmer 21st century air temperatures. Warmer headwater temperatures translate into warmer temperatures downstream.

The warmest stream temperatures are projected to be in July and August, consistent with the general increase in summer air temperatures in the MACA forcings. Historically, an average

peak stream temperature of approximately 15.3 °C occurred in August (Table 11). Beginning in the 2025 climate normal in each emissions scenario, average July stream temperatures exceed average August stream temperatures, even though average August air temperatures in the MACA forcings are projected to be slightly higher than July air temperatures.

At the Ecology gauge, July temperatures increase by 4.0 °C and August temperatures increase by only 1.8 °C under the RCP 8.5 emissions scenario in 2075. Freeman (2019) determined that the warmest stream temperatures at the North Fork gauge are projected to occur in July as well (see section 4.4 below).

Increased air temperatures and decreased snowmelt will result in warmer headwater temperatures during spring. Headwater temperatures are projected to increase anywhere from 6 °C to 8 °C in July by the end of the century under the CSIRO-Mk3-6-0 GCM under RCP 8.5 (Figure 10). A projected lower snowmelt and decreased summer precipitation will also result in lower streamflows and warmer temperatures downstream. Slower, shallower water reaches equilibrium and responds more quickly to heat inputs and increasing temperatures.

Because the model outputs temperatures at three-hour time steps, it is worth it to note that the maximum temperature output on any given day may not be the true maximum temperature of that day. In the extreme emissions scenario, the average number of days per year exceeding the 16 °C 7-DADMax threshold for core summer salmon habitat, migration, and spawning will increase by 275% from historical temperatures by 2075 (Table 12). The average number of days per year exceeding the 17.5 °C 7-DADMax threshold for salmon embryo lethality will increase by approximately 420% from historical temperatures by 2075 (Table 13). The average number of days per year exceeding the 22 °C 7-DADMax threshold for adult salmon lethality increased from an average of zero days per year to 43 days per year by 2075 under the extreme climate

scenario (Table 14). Single day peak temperature of 23-25 °C can be lethal to salmonids that are not yet acclimated to warm waters. The first instance of a peak modeled daily maximum temperature of 23 °C is projected to occur in July of 2080 under the HadGEM2-ES365 RCP 8.5 climate scenario, one of the most extreme scenarios. These results are consistent with habitat assessment studies, where Mantua et al. (2010) found that the mainstem Stillaguamish River may reach lethal temperatures by the 2080s. Krosby et al. (2016) found that Chinook salmon and steelhead trout will have greatly increased vulnerability to increasing temperature and discharge changes by the 2050s. Cao et al. (2016) projected that, under RCP 4.5, the annual maximum 7-DADMax may exceed 24 °C by 2050 and that there may be more than 50 days per year that exceed 20 °C by the middle of the century.

Cao et al. (2016) used uniform riparian zone characteristics along all stream segments of the Stillaguamish River basin, but I was able to improve on that aspect of the model with characteristics specific to the South Fork basin. Cao et al. (2016) used NOAA land cover data from 2002, while I used the NOAA land cover data set from 2011. Land cover grids will be updated for future similar work and updated data sets become available. Riparian cover is very important for providing shade to streams and mitigating stream temperatures, and lidar and specific land cover and vegetation type data were improved for this project by applying methods developed by Freeman (2019). I used high-resolution lidar to determine an average tree height of 13.6 meters in the riparian zone and to quantify the extinction coefficient specific to each vegetation type (Table 1). It is also important to note that Cao et al. (2016) conducted their study at the outlet of the Stillaguamish River into the Puget Sound, and results may be more extreme than my results at the Ecology gauge along the mainstem of the South Fork. The prediction of 50 days per year exceeding a 7-DADMax of 20 °C at the outlet of the Stillaguamish River (Cao et

al. 2016) may be exaggerated by the generalized riparian characteristics. At the Ecology gauge in the South Fork basin, my results predict approximately 6 days per year exceeding the 20 °C 7-DADMax by 2050.

4.4 Comparison to North Fork

Projected streamflow trends in the South Fork basin are similar to those predicted in the North Fork basin (Freeman, 2019). The South Fork basin is smaller and generally has lower streamflow than the North Fork historically, but both basins and streams exhibit similar projected trends. By the 2075 climate normal, winter peak flows increased by as much as 75% and the basin-wide SWE decreases by as much as one order of magnitude in both basins.

In terms of projected stream temperatures, both the North Fork and the South Fork have similar increasing trends, although the North Fork stream temperatures at the Ecology gauge are projected to be slightly warmer. Both streams have the highest monthly increases in stream temperature in June due to a reduction in snowmelt. My results project that July will be the warmest month in the South Fork basin, which is consistent with the findings of Freeman (2019). Historical simulations show that stream temperatures in the South Fork basin are higher than the North Fork basin, with more days per year exceeding the 16 °C and 17.5 °C DAD-Max temperature thresholds. By the end of the century, the North Fork is projected to be warmer than the South Fork every month of the year. The exact reason for the change is unknown, but the two basins are unique in size, shape, mainstem valley widths, and aspects, and the areas contributing to streamflow and temperature at the respective Ecology gauges in the two forks are different. One cause in warming between the two basins is likely due to the differences in the general orientations of the North Fork and South Fork basins. Using ArcGIS, I quantified and compared the aspects and percentage of streams exposed to daytime solar inputs. The South Fork basin is

generally east-west trending and the river is restricted to a narrower valley with a lesser degree of southerly aspects; as such, stream segments begin to receive less solar radiation after the summer solstice. Above the Ecology gauge, the North Fork has 20% more stream kilometers with a southerly aspect and therefore receives more solar radiation overall in the late summer than the South Fork (Figure 13).

Although both basins have similar topographic relief, the North Fork and South Fork basins differ in their mainstem valley physiographic characteristics. The North Fork valley was once the outlet for the upper Skagit River, the Suiattle River, and the Sauk River and is now much wider than the mainstem valley of the South Fork. Because the North Fork valley is wider with more sediment deposits, there may be more cool groundwater influence. Freeman (2019) addresses this by noting that her projected summer stream temperatures may be higher than what may actually occur because the model does not sufficiently simulate the influence of groundwater. Because the South Fork valley is much narrower than the North Fork valley, it is possible that there is less groundwater influence in the South Fork from valley sediments, which would contribute to potentially warmer stream temperatures. This difference in channel morphology, in addition to the general orientation of the basin may explain the results projected by the models.

The South Fork Chinook salmon population are genetically unique from the North Fork Chinook salmon population. South Fork Chinook populations tend to migrate upstream and spawn from mid-September to mid-October, which is later than the North Fork Chinook salmon migration and spawning patterns (SIRC, 2005). Fall run Chinook salmon mainly utilize Jim Creek and lower parts of the South Fork Stillaguamish River (SIRC, 2005; Figure 12). Jim Creek has already experienced issues with low streamflows in the late summer and early fall. Salmon were not able to use the stream at all in 1979 (WSDOE, 1981). The stream temperature in the

mainstem of Jim Creek is projected to increase by 3 to 5 °C by the 2075 climate normal, the least affected region in the South Fork basin (Figure 10). This may be a result of Jim Creek being protected by mixed forests of deciduous and coniferous trees. Remnants of a spring Chinook salmon run can still be found farther upstream and in the Canyon Creek subbasin (SIRC, 2005; Figure 12). A fish ladder built in 1954 at Granite Falls allows for easier passage for fish migrating farther upstream the mainstem of the South Fork. Clear-cut logging contributes to rapid changes in the streambed of Canyon Creek, resulting in the filling of holding pools that have been critical refugia for migrating salmon (WSDOE, 1981). Stream temperatures in the mainstem of Canyon Creek are projected to increase by at least 4 °C by the 2075 climate normal, with tributary temperatures projected to increase by 5 to 8 °C (Figure 10). This may be another result of continued logging higher up in the sub-basin or the number of slopes with southerly aspects receiving more solar radiation during early- to mid-summer. Further studies on the impact of solar radiation and projected impact of reforestation could help to inform river managers of regions to focus restoration efforts. River managers may find it beneficial to record stream temperature continuously in Jim Creek, Canyon Creek, and the mainstem of the South Fork to observe changing trends in the timing and magnitudes of stream temperature in the near future.

Even in warm streams, salmon can find refuge in cool pools along their migration corridors and can adapt somewhat to warmer stream temperatures by utilizing these deep, cool pools. These sites may be points of cool groundwater input to the stream or hyporheic exchange. The DHSVM and RBM cannot fully capture specific points of cool water input to the stream, so it is difficult to predict the availability of cold-water refugia in warm streams.

4.5 Uncertainty and Model Limitations

Like all physical models, the DHSVM and RBM each have their own model limitations, particularly when it comes to natural, physical processes on finer scales. Currently the RBM is limited in its ability to consider variability in hyporheic flow and the influence of groundwater recharging to or discharging from a stream. The hyporheic zone of the stream is where groundwater and surface water mix, and water is often cooler in this zone than at the surface of the stream. The hyporheic zone is important for creating cool pools for fish spawning habitats. The RBM sets the groundwater temperature equal to the temperature of the headwaters and does not consider outflow or inflow of groundwater to and from a stream at varying points along reaches.

The vegetation input grid for the DHSVM is constant for the entirety of the model runtime, so changes in vegetation into the 21st century are not taken into account. Vegetation could change due to growth or loss from planting, logging, or wildfires. This could result in the model underestimating or overestimating evapotranspiration and shading from the riparian zone. The input file is also limited by a 50-meter resolution and may not accurately reflect finer real-world characteristics of the South Fork basin. The topography of the South Fork basin is complex and can vary significantly in a small area.

The historical and projected climate data have been downscaled from a coarse resolution to a finer resolution on a small scale, which results in unavoidable imperfections. In the hindcast, winter and spring peak flows are not captured due to the format of the gridded Livneh data, which disaggregates daily meteorological data into three-hour intervals. Precipitation is distributed over 24 hours and does not represent a shorter, more powerful storm and correlating increase in streamflow. Monthly GCM data are bias-corrected and disaggregated to small-scale,

three-hour time steps, but not all biases can be corrected. For example, Freeman (2019) discovered a low-precipitation bias in the projected climate data. The UW-CIG are working to improve these meteorological data sets, which will eventually allow for better assessment of the historical, current, and future states of the basin. The projected streamflows and stream temperatures are not intended to be accurate on a day-by-day basis, but instead are intended to show general trends of what river managers can expect to see through the rest of the century.

4.6 Future Work

River managers may benefit from modeling the Jim Creek and Canyon Creek sub-basins individually to better predict changes in streamflow and stream temperature specific to those regions. It would also be important to model future climate impacts on Pilchuck Creek and the mainstem of the Stillaguamish River downstream of the confluence of the North and South forks. The version of RBM used in the project only predicts temperature to the mouth of the South Fork basin and not beyond that point. Improvements could be made to this project by modeling the entire Stillaguamish River basin as a whole. New versions of the RBM could model the entire basin with Mohseni and Leopold parameters specific to each sub-basin, including the North Fork, South Fork, Pilchuck Creek, and the mainstem out to the Puget Sound. This could potentially use predicted stream temperatures upstream to predict future stream temperatures along the mainstem downstream of the confluence of the North and South forks.

5.0 Conclusions

Projected warming air temperatures into the 21st century and projected modeling with the DHSVM project decreased future snowpack, increased winter rainfall and streamflow, and decreased summer precipitation, which would all result in lower spring and summer streamflows. The effects of a warming climate will be more pronounced later in the century and under the extreme emissions scenario (RCP 8.5). Even if actions are taken now to reduce greenhouse gas emissions, the effects of that will likely not be noticeable until at least the middle of the century. More winter rainfall will cause higher runoff and streamflows, which will cause increased sediment loading to the river. This will endanger salmon habitat and increase winter flood risks for communities within the Stillaguamish River basin. A more detailed risk assessment for winter flooding would require more thorough analysis of peak flows. The influence of groundwater on streamflow is not fully captured in the DHSVM, and so streamflows in the spring and early summer may be underestimated as snowpack decreases in the future, but the simulated streamflow can be considered a "worst-case scenario." Efforts to protect salmonids and habitats could benefit from a more detailed analysis of localized groundwater discharge that creates cold water pools for migrating salmon.

Stream temperatures can be expected to increase into the 21st century in correlation with projected increasing air temperatures and changes in streamflow and snowpack trends. The greatest increase in stream temperature is projected to occur between May and July as a result of less snowpack and less spring runoff. The warmest month for stream temperatures moves from August to July by the 2025 climate normal, with more noticeable differences between July and August temperatures by 2050 and 2075. Ecology freshwater quality thresholds for adult salmon migration and spawning and embryo and adult lethality will be increasingly exceeded through

the end of the century, with as many as 108 days per year that exceed the 22 °C adult salmon lethality threshold in the most extreme climate scenario in this study (CanESM2 RCP 8.5). WSDOE recommends cold water refugia frequent enough that a fish may not be entrained in water above 33 °C for more than 2 seconds at any time to avoid instantaneous lethality. The RBM predicts that the river will reach a lethal temperature of 23 °C at the Ecology gauge by July of 2080. The model outputs simulated stream temperature at three-hour intervals, so it is possible that there may be days with temperatures around or above 23 °C before that or farther downstream of the Ecology gauge as well. The already endangered Chinook salmon and steelhead trout will be increasingly susceptible to warming air and stream temperatures through the 21st century.

6.0 Works Cited

Abatzoglou, J.T., and Brown, T.J., 2012, A comparison of statistical downscaling methods suited for wildfire applications: International Journal of Climatology, v. 32, p. 772–780.

Bergendorf, D., 2002, The Influence of In-stream Habitat Characteristics on Chinook Salmon (*Oncorhynchus tshawytscha*): National Oceanic and Atmospheric Administration, National Marine Fisheries Service.

Boone, Chad. "WWII Antenna Replaced at Jim Creek." *Northwest Navy Life*, 6 Dec. 2012, archive.kitsapsun.com/northwest-navy-life/wwii-antenna-replaced-at-jim-creek-ep-492327218-356383931.html.

Cao, Q., Sun, N., Yearsley, J., Nijssen, B., Lettenmaier, D.P., 2016, Climate and land cover effects on the temperature of Puget Sound streams: Hydrological Processes, v. 30, p. 2286-2304.

Cuo, L, D.P. Lettenmaier, B. V. Mattheussen, P.Storck and M. Wiley, 2008: Hydrological prediction for urban watersheds with the Distributed Hydrology-Soil-Vegetation Model, *Hydrological Processes*, 22(21) 4205-4213 DOI: 10.1002/hyp.7023.

Dickerson-Lange, S.E., and Mitchell, R., 2014, Modeling the effects of climate change projections on streamflow in the Nooksack River basin, Northwest Washington: Hydrological Processes, v. 28, p. 5236-5250.

Elsner, M., Cuo, L., Voisin, N., Deems, J., Hamlet, A., Vano, J., Mickelson, K., Lee, S., and Lettenmaier, D. (2010). Implications of 21st Century Climate Change for the Hydrology of Washington State. Climatic Change. 102. 225-260. 10.1007/s10584-010-9855-0.

Freeman, K., 2019, Modeling the Effects of Climate Variability on Hydrology and Stream Temperatures in the North Fork of the Stillaguamish River. *WWU Graduate School Collection.* 855. https://cedar.wwu.edu/wwuet/855.

Hansen, J., Nazarenko, L., Ruedy, R., Sato, M., Willis, J., Del Genio, A., Koch, D., Lacis, A., Lo, K., Menon, S., and others, 2005, Earth's Energy Imbalance: Confirmation and Implications: Science, v. 308, p. 1431–1435.

Killebrew, K., Graybill, K., Freeman, K., (2018, October 9-11). An Alternative Method for Mounting Tidbit Temperature Sensors. Northwest Climate Conference 2018, Boise, ID, United States. https://www.fs.fed.us/rm/boise/AWAE/projects/stream_temp/downloads/19underwater-drill-thermograph-installation_poster.pdf

Krosby, M., Morgan, H., Case, M., and Whitely Binder, L., 2016, Stillaguamish Tribe Natural Resources Climate Change Vulnerability Assessment: Climate Impacts Group, University of Washington, https://cig.uw.edu/news-and-events/publications/stillaguamish-tribe-natural-resources-climate-change-vulnerabilityassessment.

Lee, S-Y., A. Fullerton, N. Sun, C. Torgersen (2020). Projecting spatiotemporally explicit effects of climate change on stream temperature: A model comparison and implications for coldwater fishes. Journal of Hydrology 588. DOI: https://doi.org/10.1016/j.jhydrol.2020.125066

Littell, J.S., Elsner, M.M., Whitely Binder, L.C., and Snover, A. (Eds.), 2009, The Washington Climate Change Impacts Assessment: Evaluating Washington's Future in a Changing Climate - Executive Summary, in The Washington Climate Change Impacts Assessment: Evaluating Washington's Future in a Changing Climate, Seattle, Washington, Climate Impacts Group, University of Washington, http://www.cses.washington.edu/db/pdf/wacciaexecsummary638.pdf

Livneh, B., Rosenberg, E.A., Lin, C., Nijssen, B., Mishra, V., Andreadis, K.M., Maurer, E., and Lettenmaier, D.P., 2013, A Long-Term Hydrologically Based Dataset of Land Surface Fluxes and States for the Conterminous United States: Update and Extensions: Journal of Climate, v. 26, p. 9384–9392, doi: 10.1175/JCLI-D-12-00508.1.

Mantua, N., Tohver, I., and Hamlet, A. (2010). Climate Change Impacts on Streamflow Extremes and Summertime Stream Temperature and Their Possible Consequences for Freshwater Salmon Habitat in Washington State. Climatic Change. 102. 187-223. 10.1007/s10584-010-9845-2.

Mauger, G., Lee, S., Bandaragoda, C., Serra, Y., and Won, J., 2016, Refined Estimates of Climate Change Affected Hydrology in the Chehalis Basin: Report prepared for Anchor QEA, LLC. Climate Impacts Group, University of Washington, Seattle. doi, v. 10.

Mauger, G.S., J.S. Won, K. Hegewisch, C. Lynch, R. Lorente Plazas, E. P. Salathé Jr., 2018. New Projections of Changing Heavy Precipitation in King County. Report prepared for the King County Department of Natural Resources. Climate Impacts Group, University of Washington, Seattle.

Morgan, H., R. Norheim, and M. Krosby. 2017. Maps of Climate and Hydrologic Change for the Nooksack River Watershed. Climate Impacts Group, University of Washington.

Moriasi, D. N., Arnold, J. G., Van Liew, M. W., Bingner, R. L., Harmel, R. D., Veith, T. L.; "Model Evaluation Guidelines for Systematic Quantification of Accuracy in Watershed Simulations." *Transactions of the ASABE*, vol. 50, no. 3, 2007, pp. 885-900., dio: 10.13031/2013.23153.

Moriasi, D., Gitau, M., Pai, N., and Daggupati, P., 2015a, Hydrologic and Water Quality Models: Performance Measures and Evaluation Criteria: Transactions of the ASABE (American Society of Agricultural and Biological Engineers), v. 58, p. 1763–1785, doi:10.13031/trans.58.10715.

Moriasi, D. N., Zeckoski, R. W., Arnold, J. G., Baffaut, C. B., Malone, R. W., Daggupati, P., Guzman, J. A., Saraswat, D., Yuan, Y., Wilson, B. W., Shirmohammadi, A., Douglas-Mankin, K. R., 2015b, Hydrologic and water quality models: Key calibration and validation topics. *Transactions of the ASABE*, *58*(6), 1609-1618. https://doi.org/10.13031/trans.58.11075

Mote, P.W., and Salathé, E.P., 2010, Future climate in the Pacific Northwest: Climatic Change, v. 102, p. 29–50, doi: 10.1007/s10584-010-9848-z.

Mote, P., Snover, A., Capalbo, S., Eigenbrode, S., Glick, P., Littell, J., Raymondi, R., and Reeder, S., 2014, Ch. 21: Northwest: Climate Change Impacts in the United States: The Third National Climate Assessment, JM Melillo, Terese (TC) Richmond, and GW Yohe, Eds., US Global Change Research Program, p. 487–513.

Murphy, A., 1988. Skill Scores Based on the Mean Square Error and Their Relationships to the Correlation Coefficient: Monthly Weather Review, v.116, pp. 2417-2424.

Murphy, R., 2016, Modeling the Effects of Forecasted Climate Change and Glacier Recession on Late Summer Streamflow in the Upper Nooksack River Basin: WWU Masters Thesis Collection, http://cedar.wwu.edu/wwuet/461.

Nash, J.E., and Sutcliffe, J.V., 1970, River flow forecasting through conceptual models part I — A discussion of principles: Journal of Hydrology, v. 10, p. 282–290, doi: 10.1016/0022-1694(70)90255-6.

PRISM Climate Group, 2014, Average Annual Precipitation (1981-2010), Washington: Oregon State University, http://prism.oregonstate.edu/projects/gallery_view.php?state=WA.

Rupp, D.E., Abatzoglou, J.T., Hegewisch, K.C., and Mote, P.W., 2013, Evaluation of CMIP5 20th century climate simulations for the Pacific Northwest USA: Journal of Geophysical Research: Atmospheres, v. 118, p. 2013JD020085, doi: 10.1002/jgrd.50843.

Snover, A.K, G.S. Mauger, L.C. Whitely Binder, M. Krosby, and I. Tohver. 2013. Climate Change Impacts and Adaptation in Washington State: Technical Summaries for Decision Makers. State of Knowledge Report prepared for the Washington State Department of Ecology. Climate Impacts Group, University of Washington, Seattle.

Stillaguamish Implementation Review Committee (SIRC). 2005. Stillaguamish Watershed Chinook Salmon Recovery Plan. Published by Snohomish County Department of Public Works, Surface Water Management Division. Everett, WA, https://www.snohomishcountywa.gov/Archive.asp?ADID=2163 (accessed January 2020).

Sun, N., Yearsley, J., Voisin, N., and Lettenmaier, D.P., 2015, A spatially distributed model for the assessment of land use impacts on stream temperature in small urban watersheds: Hydrological Processes, v. 29, p. 2331-2345.

Tohver I, Hamlet A. 2010. Impacts of 21st century climate change on hydrologic extremes in the Pacific Northwest region of North America. Columbia Basin Climate Change Scenarios Project (PI: Alan F. Hamlet), University of Washington, Seattle, WA; 31 pp. http://www.hydro.washington.edu/2860/report

Turnipseed, D.P., and Sauer, V.B., 2010, Discharge measurements at gaging stations: U.S. Geological Survey Techniques and Methods book 3, chap. A8, 87 p. (Also available at https://pubs.usgs.gov/tm/tm3-a8/.)

Truitt, Stephanie E., 2018, Modeling the Effects of Climate Change on Stream Temperature in the Nooksack River Basin. WWU Graduate School Collection. 642. https://cedar.wwu.edu/wwuet/642

Vano, J.A., Voisin, N., Cuo, L., Hamlet, A.F., Elsner, M.M., Palmer, R.N., Polebitski, A., and Lettenmaier, D.P., 2010, Climate change impacts on water management in the Puget Sound region, Washington State, USA: Climatic Change, v. 102, p. 261–286, doi:10.1007/s10584-010-9846-1.

Vano, J. A., B. Nijssen, and D. P. Lettenmaier (2015), Seasonal hydrologic responses to climate change in the Pacific Northwest, *Water Resources. Res.*, 51, 1959–1976, doi:10.1002/2014WR015909.

Wigmosta, M. S., Nijssen, B., Storck, P., 1994: The Distributed Hydrology Soil Vegetation Model, In Mathematical Models of Small Watershed Hydrology and Applications, V. P. Singh, D. K. Frevert, eds., Water Resource Publications, Littleton, CO., p. 7-42.

WSDOE, Washington State Department of Ecology, 1981, Stillaguamish River Basin Instream Resources Protection Program, https://fortress.wa.gov/ecy/publications/publications/8111004.pdf

WSDOE, Washington State Department of Ecology, 2002, Evaluating Standards for Protecting Aquatic Life in Washington's Surface Water Quality Standards: Temperature Criteria.

WSDOE, Washington State Department of Ecology, 2004, Stillaguamish River Watershed Temperature Total Maximum Daily Load Study.

WSDOE, 2015, Stillaguamish Temperature TMDL Adaptive Assessment and Implementation Report, Washington State Department of Ecology.

WSDOE, Washington State Department of Ecology, 2018, S.F. Stillaguamish R. at Jordan Rd. Bridge, https://fortress.wa.gov/ecy/eap/flows/station.asp?sta=05A105.

Yearsley, J.R., 2009, A semi-Lagrangian water temperature model for advection-dominated river systems: Water Resources Research, v. 45, p. 1–19, doi:10.1029/2008WR007629.

Yearsley, J.R., 2012, A grid-based approach for simulating stream temperature: ResearchGate, v. 48, p. 1–15, doi:10.1029/2011WR011515.

7.0 Tables

Table 1. Riparian conditions input in DHSVM for use in RBM temperature simulations, the method of parameter selection for present day vegetation conditions, and comparison to parameters used by Cao et al. (2016).

Parameter	Method	Description	Range	Cao value
Tree height	Estimated for each individual segment with a python script and ArcGIS	Lidar data were used to determine the average tree height in a 10-meter buffer along each stream segment.	0 – 31.1 m (13.6 m basin-wide average)	10 m
Buffer width	Basin-wide average	Based on the value used by Freeman, 2019.	10 m	5 m
Extinction coefficient	Manually estimated from LAI values of land cover file	In ArcGIS, I extracted a land cover file that only included the cells along the stream network. I populated the rveg file with the appropriate average extinction coefficient for each stream segment based on input values in the DHSVM configuration file.	0 – 0.125	0.08
Overhang coefficient	Basin-wide average	This value was used by Cao et al. (2016).	0.01	0.01
Canopy-bank distance	Basin-wide average	This value was used by Cao et al. (2016).	0 m	0 m
Channel width	Manually estimated based on stream segment type	Mainstem widths were estimated from Google Earth Pro imagery. All tributaries were assigned a value of 10 m.	Mainstem 10-70 m; tributaries 10 m	

Table 2. Statistical tests for calibrating and evaluating hydrologic models, where

O = observed data

P = predicted data

Test		**Calculation**	**Satisfactory values**	
NSE	Nash-Sutcliffe Efficiency	$NSE = 1.0 - \frac{\sum_{i=1}^{N}(O_i - P_i)^2}{\sum_{i=1}^{N}(O_i - \bar{O})^2}$	> 0.50	NSE is a widely accepted skill score based on mean squared error of the model compared to the observed data (Murphy, 1988)
R^2		$R^2 = \left\{\frac{\sum_{i=1}^{N}(O_i - \bar{O})(P_i - \bar{P})}{[\sum_{i=1}^{N}(O_i - \bar{O})^2]^{0.5}[\sum_{i=1}^{N}(P_i - \bar{P})^2]^{0.5}}\right\}^2$	> 0.60	Describes the portion of total variance in the observed data that is explained by the model (Moraisi, 2015)
RSR	RMSE-observations standard deviation ratio	$RSR = \frac{RMSE}{STDEV_{obs}} = \frac{\sqrt{\sum_{i=1}^{N}(O_i - P_i)^2}}{\sqrt{\sum_{i=1}^{N}(O_i - \bar{\bar{O}})^2}}$	< 0.70	Root mean square error divided by the standard deviation (ASABE, 2017)
PBIAS	Percent bias	$PBIAS = \frac{\sum_{i=1}^{N}(O_i - P_i) * 100}{\sum_{i=1}^{N}(O_i)}$	< 15%	Measures the average tendency of the simulated data to be larger or smaller than their observed counterparts (ASABE, 2017)

Table 3. GCMs used to project streamflow and stream temperature in representative concentration pathway scenarios 4.5 and 8.5, as outlined by Rupp et al. (2013).

Model Name	**Model Country**	**Model Agency**	**Ensemble Used**	**Resolution (lat x long)**
Bcc-csm1-1-m	China	Beijing Climate Center, China Meteorological Administration	r1i1p1	2.7906 x 2.8125
CanESM2	Canada	Canadian Centre for Climate Modeling and Analysis	r1i1p1	2.7906 x 2.8125
CCSM4	USA	National Center of Atmospheric Research	r6i1p1	0.9424 x 1.25
CNRM-CM5	France	National Centre of Meteorological Research	r1i1p1	1.4008 x 1.40625
CSIRO-Mk3-6-0	Australia	Commonwealth Scientific and Industrial Research Organization/Queensland Climate Change Centre of Excellence	r1i1p1	1.8653 x 1.875
HadGEM2-ES	United Kingdom	Met Office Hadley Center	r1i1p1	1.25 x 1.875
HadGEM2-CC	United Kingdom	Met Office Hadley Center	r1i1p1	1.25 x 1.875
IPSL-CM5A-MR	France	Institut Pierre Simon Laplace	r1i1p1	2.5352 x 2.5
MIROC5	Japan	Atmosphere and Ocean Research Institute (The University of Tokyo), National Institute for Environmental Studies, and Japan Agency for Marine-Earth Science and Technology	r1i1p1	1.4008 x 1.40625
NorESM1-M	Norway	Norwegian Climate Center	r1i1p1	1.8947 x 2.5

Table 4. Important DHSVM calibration parameters.

Description	**Value**
Minimum rain temperature threshold	1 ºC
Maximum snow temperature threshold	1 ºC
Snow water capacity	0.03
Precipitation lapse rate	0.0005 m/m
Soil lateral conductivity	
Loamy sand	0.001 m/s
Sandy loam	0.0005 m/s
Silt	0.0005 m/s
Silty loam	0.0001 m/s
Soil vertical conductivity	
Loamy sand	0.005 m/s
Sandy loam	0.005 m/s
Silt	0.005 m/s
Silty loam	0.05 m/s
Soil maximum depth	4 meters
Soil minimum depth	0.76 meters
Stream network source area	330,000 m^2

Table 5. Variable temperature lapse rates by month for meteorological stations (Livneh nodes) 1-4.

Month	**Temperature lapse rate (°C/m)**
January	-0.0055
February	-0.0055
March	-0.0055
April	-0.0045
May	-0.003
June	-0.003
July	-0.003
August	-0.003
September	-0.003
October	-0.0045
November	-0.0055
December	-0.0055

Table 6. Variable temperature lapse rates by month for meteorological station (Livneh node) 5.

Month	**Temperature lapse rate (°C/m)**
January	-0.005
February	-0.005
March	-0.005
April	-0.003
May	-0.003
June	-0.003
July	-0.003
August	-0.003
September	-0.003
October	-0.004
November	-0.005
December	-0.005

Table 7. Performance evaluation criteria of the calibration of the DHSVM to streamflow measured at the Ecology stream gauge (05A105) from water years 2004 to 2009.

	All data		**May – September only**	
	Daily mean	Monthly mean	Daily mean	Monthly mean
NSE	0.464	0.854	0.618	0.807
R^2	0.477	0.895	0.686	0.945
RSR	0.732	0.378	0.617	0.43
PBIAS	-13.4	-13.3	-24.1	-24.1
PEC rating	Very Good	Good	Satisfactory	Not satisfactory

Table 8. Mohseni and Leopold parameters used in the calibration of RBM.

Description	**Value**
Mohseni α	22.0
Mohseni β	11.5
Mohseni γ	0.30
Mohseni μ	1.0
Mohseni smoothing	0.04
Leopold a	0.35
Leopold b	0.40
Leopold minimum depth	1.0 foot
Leopold c	0.30
Leopold d	0.40
Leopold minimum speed	1.0 foot/second

Table 9. Performance evaluation criteria of the calibration of the RBM to stream temperature measured at the Ecology gauge (05A105) from water years 2004 to 2009.

	All data		**May – September only**	
	Daily mean	Monthly mean	Daily mean	Monthly mean
NSE	0.927	0.960	0.856	0.897
R^2	0.928	0.961	0.875	0.925
RSR	0.270	0.200	0.380	0.321
PBIAS	1.3	1.2	0.8	0.8

PEC rating	Very Good	Good	Satisfactory	Not satisfactory

Table 10. Modeled monthly median streamflow in cubic meters per second (cms) at the Ecology gauge (ID 05A105) in the South Fork Stillaguamish River for median GCM results over 30 years surrounding 2025, 2050, 2075, and the historic (hindcast) period.

Month	**Historic (cms)**	**2025**		**2050**		**2075**	
		RCP 4.5	RCP 8.5	RCP 4.5	RCP 4.5	RCP 8.5	RCP 4.5
January	38.9	46.3	52.3	56.2	56.7	58.6	62.9
February	32.3	39.0	41.4	42.4	44.5	47.3	52.0
March	37.2	43.0	43.0	45.3	45.6	45.8	47.1
April	41.4	43.5	42.9	41.4	42.3	39.3	37.5
May	43.4	36.6	35.9	31.4	31.2	28.3	24.2
June	33.0	25.3	25.1	20.8	19.7	18.1	14.4
July	17.7	12.5	12.6	9.8	9.2	8.8	7.5
August	9.3	6.8	6.7	5.7	5.3	5.2	4.7
September	7.7	6.6	6.8	5.8	5.2	5.3	4.7
October	18.7	20.7	19.3	19.7	17.8	19.5	19.2
November	52.3	52.8	53.3	55.0	57.9	59.8	60.4
December	38.2	46.8	49.8	57.6	59.1	60.2	67.9

Table 11. Modeled monthly median stream temperature in degrees Celsius at the Ecology gauge (ID 05A105) in the South Fork Stillaguamish River for median GCM results over 30 years surrounding 2025, 2050, 2075, and the historic (hindcast) period.

Month	**Historic (°C)**	**2025**		**2050**		**2075**	
		RCP 4.5	RCP 8.5	RCP 4.5	RCP 8.5	RCP 4.5	RCP 8.5
January	3.3	3.4	3.4	3.6	3.7	3.8	4.4
February	3.8	4.0	3.9	4.3	4.4	4.6	5.5
March	4.5	4.7	4.9	5.3	5.4	5.9	6.7
April	6.1	6.9	6.9	7.3	7.5	7.9	9.1
May	8.2	9.1	9.2	10.0	10.5	11.0	13.1
June	10.1	12.0	12.2	13.8	14.6	14.9	16.5
July	14.1	16.0	16.2	16.8	17.2	17.3	18.1
August	15.3	15.9	16.0	16.3	16.5	16.6	17.1
September	13.0	13.8	13.8	14.3	14.6	14.6	15.2
October	8.9	9.7	10.0	10.6	11.2	11.1	12.3
November	4.4	4.9	5.0	5.5	6.0	6.0	7.0
December	3.1	3.4	3.5	3.8	3.9	4.0	4.7

Table 12. Average days per year at the South Fork Stillaguamish River Ecology gauge exceeding the 16 ºC 7-DADMax temperatures per climate normal for each median RCP emission scenario.

Emission scenario	Historic	2025	2050	2075
Moderate (RCP 4.5)	40.0	59.0	74.0	84.6
Severe (RCP 8.5)	40.0	60.4	83.4	110.3

Table 13. Average days per year at the South Fork Stillaguamish River Ecology gauge exceeding the 17.5 ºC 1-DMax temperatures per climate normal for each median RCP emission scenario.

Emission scenario	Historic	2025	2050	2075
Moderate (RCP 4.5)	18.0	33.0	45.7	53.8
Severe (RCP 8.5)	18.0	34.2	52.8	75.9

Table 14. Average days per year at the South Fork Stillaguamish River Ecology gauge exceeding the 22 ºC 7-DADMax temperatures per climate normal for each median RCP emission scenario.

Emission scenario	Historic	2025	2050	2075
Moderate (RCP 4.5)	0	0	2	7
Severe (RCP 8.5)	0	0	8	43

8.0 Figures

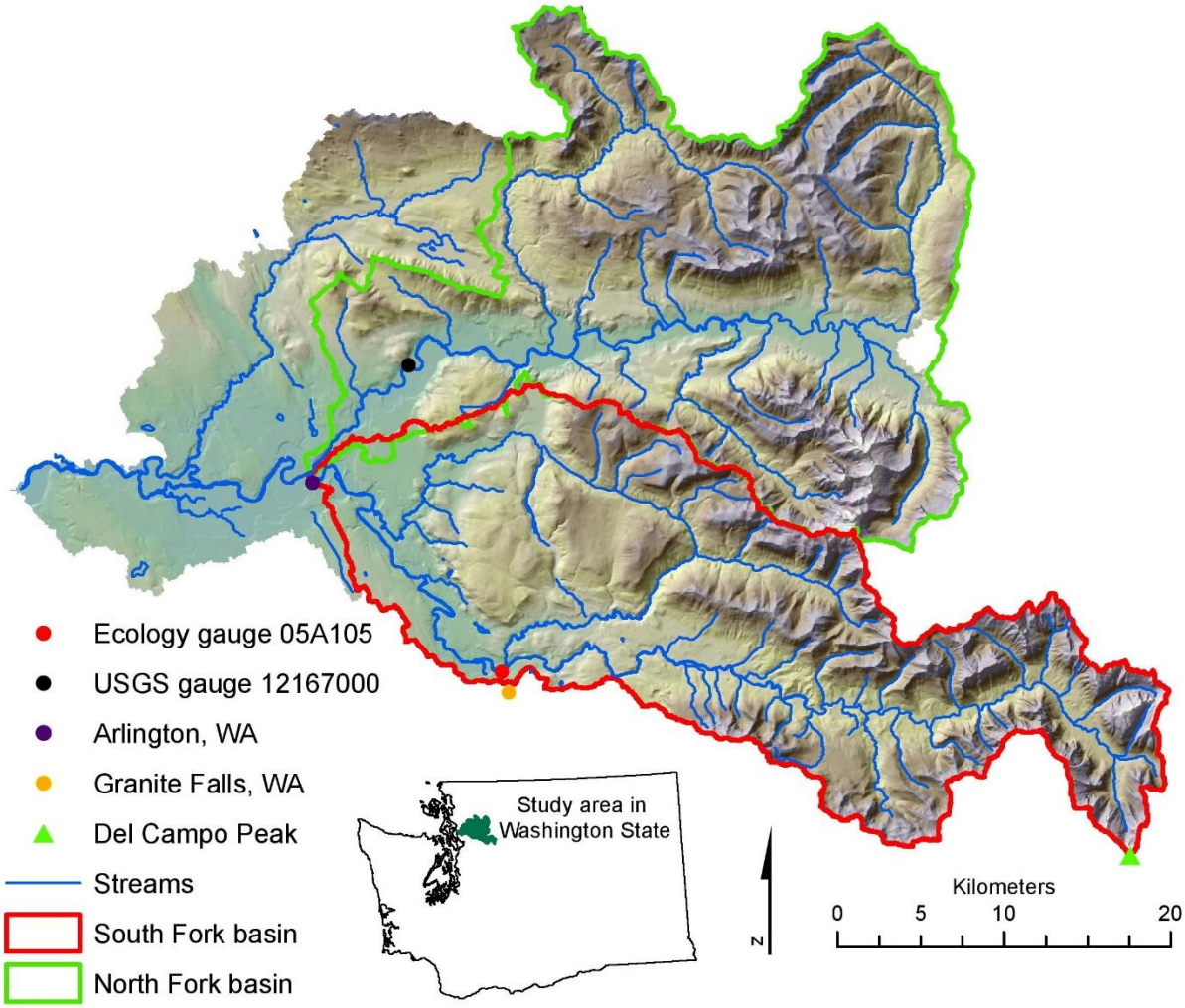

Figure 1. The Stillaguamish River basin (WRIA 5) in northwest Washington State, USA.

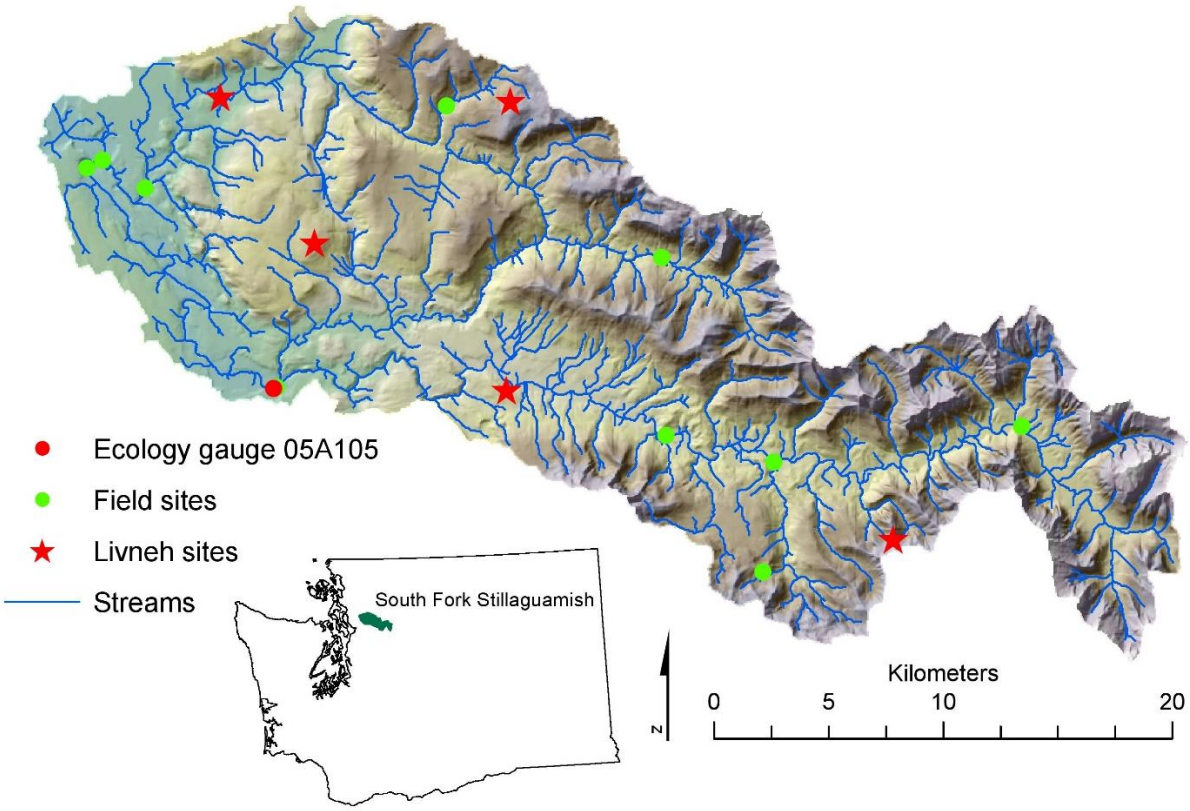

Figure 2. Field sites, Ecology stream gauge, and locations of Livneh stations in the South Fork Stillaguamish River basin in northwest Washington State.

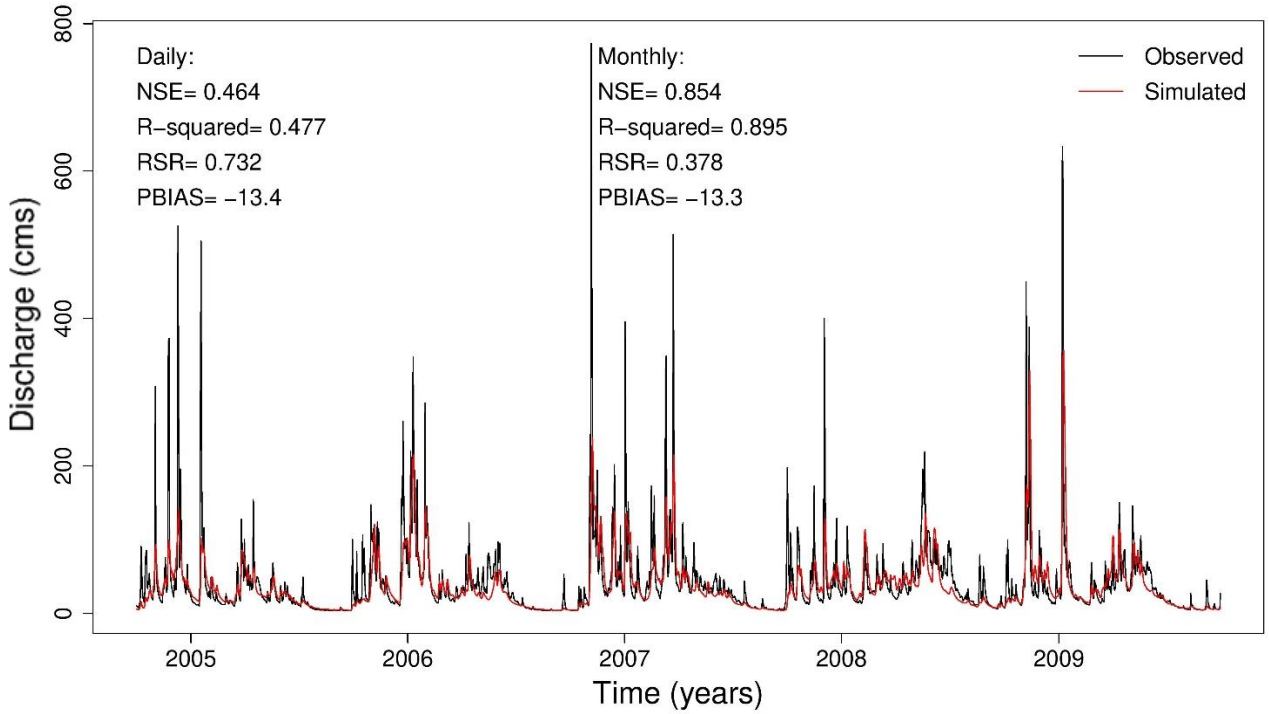

Figure 3. Calibration of the DSHVM to daily mean streamflow at the Ecology stream gauge (ID 05A105) for water years 2004 – 2009.

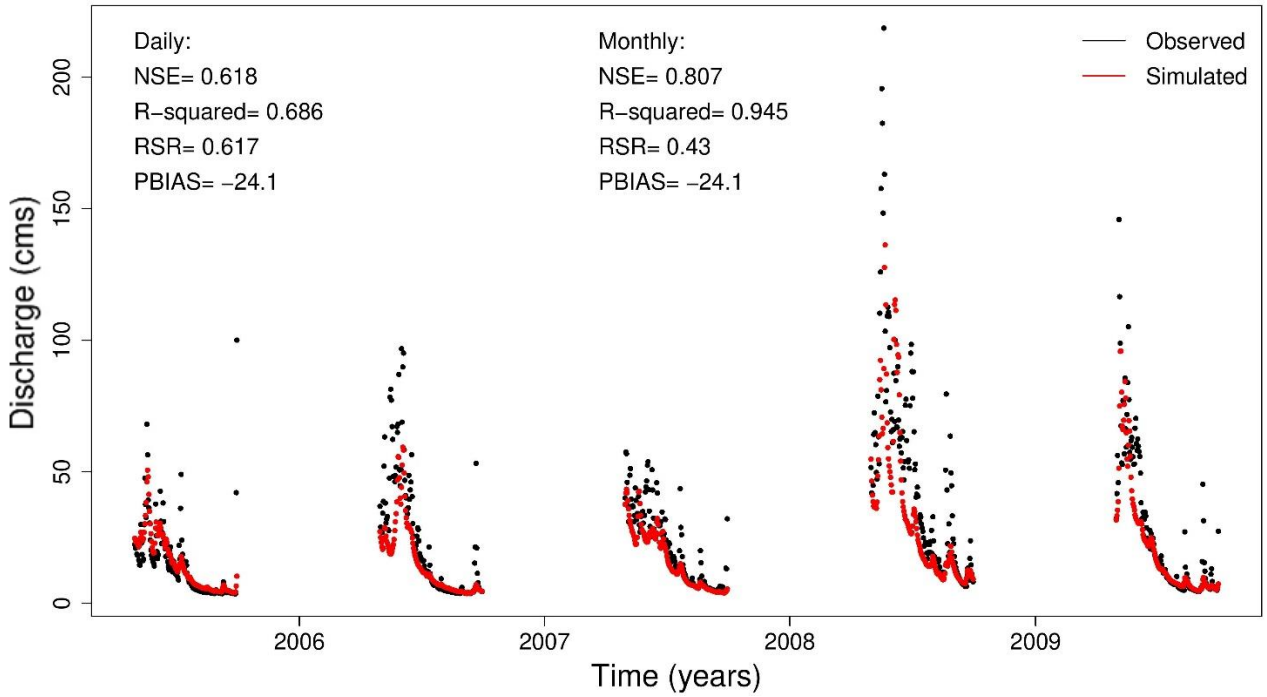

Figure 4. Calibration of the DSHVM to daily mean streamflow during low flow months May to September at the Ecology stream gauge (ID 05A105) for water years 2004 – 2009.

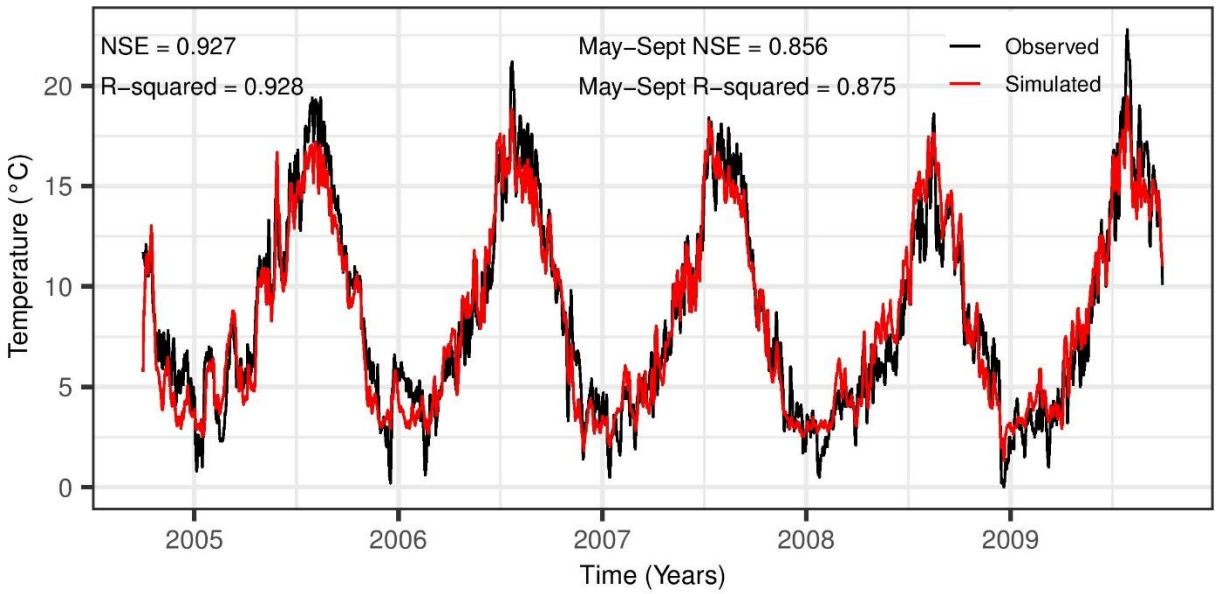

Figure 5. Calibration of the RBM to daily mean stream temperature at the Ecology gauge for water years 2004 – 2009.

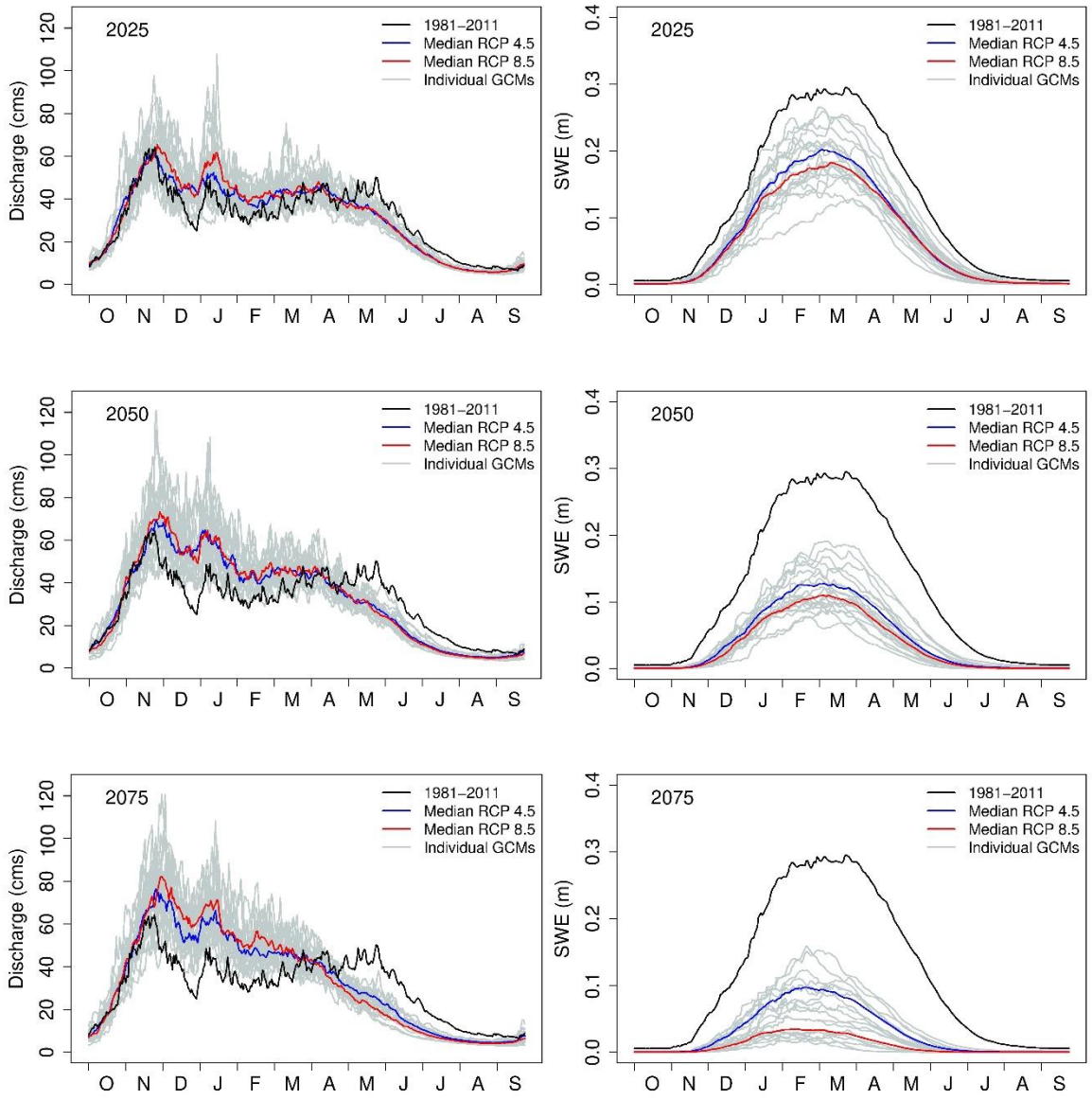

Figure 6. Monthly median streamflow and snow water equivalent over three 30-year climate normal centered on the years 2025, 2050, and 2075 at the Ecology gauge. Median hindcast values (30-year climate normal centered on the year 1996) are represented by the black line. The median RCP 4.5 values are represented by the blue line. The median RCP 8.5 values are represented by the red line. The individual GCMs are represented by the gray lines.

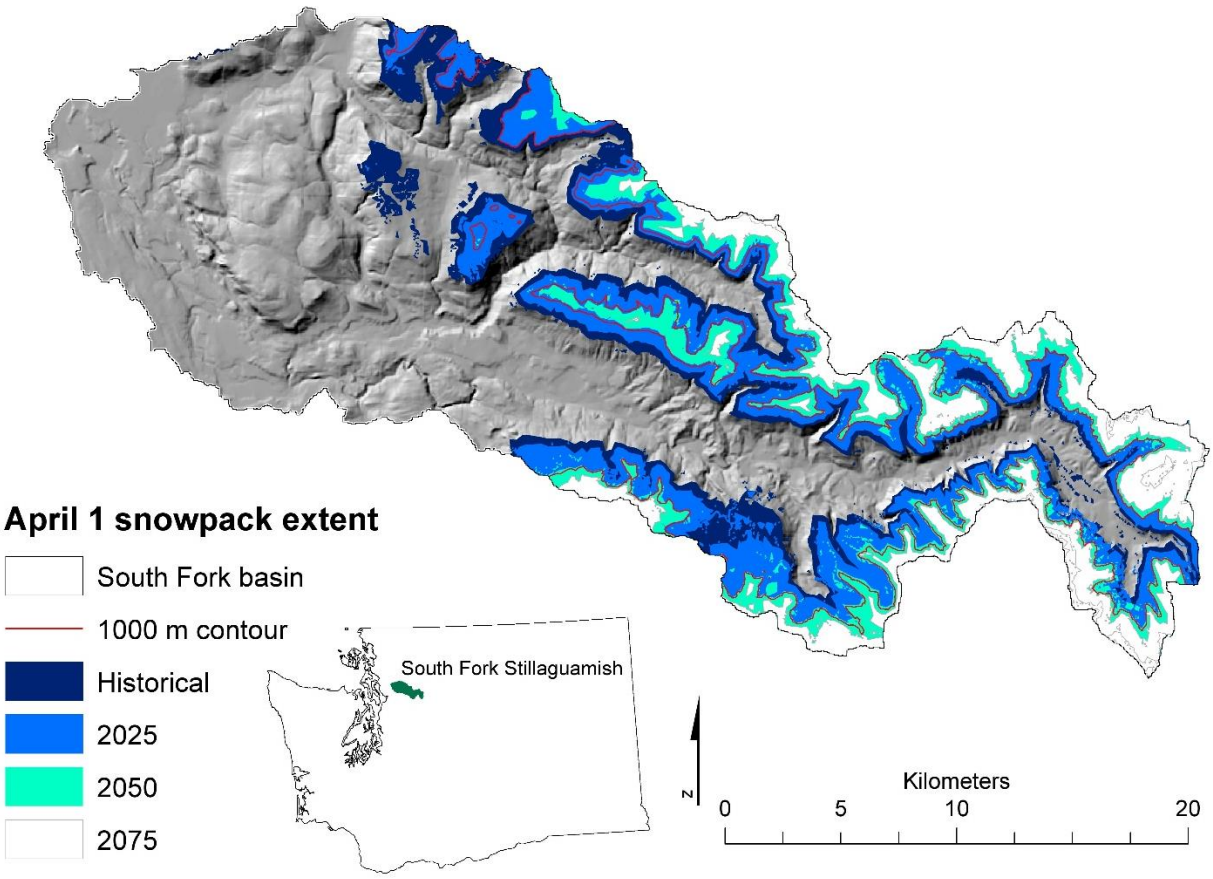

Figure 7. Average modeled April snowpack extent over three projected 30-year climate normal in the South Fork Stillaguamish River basin.

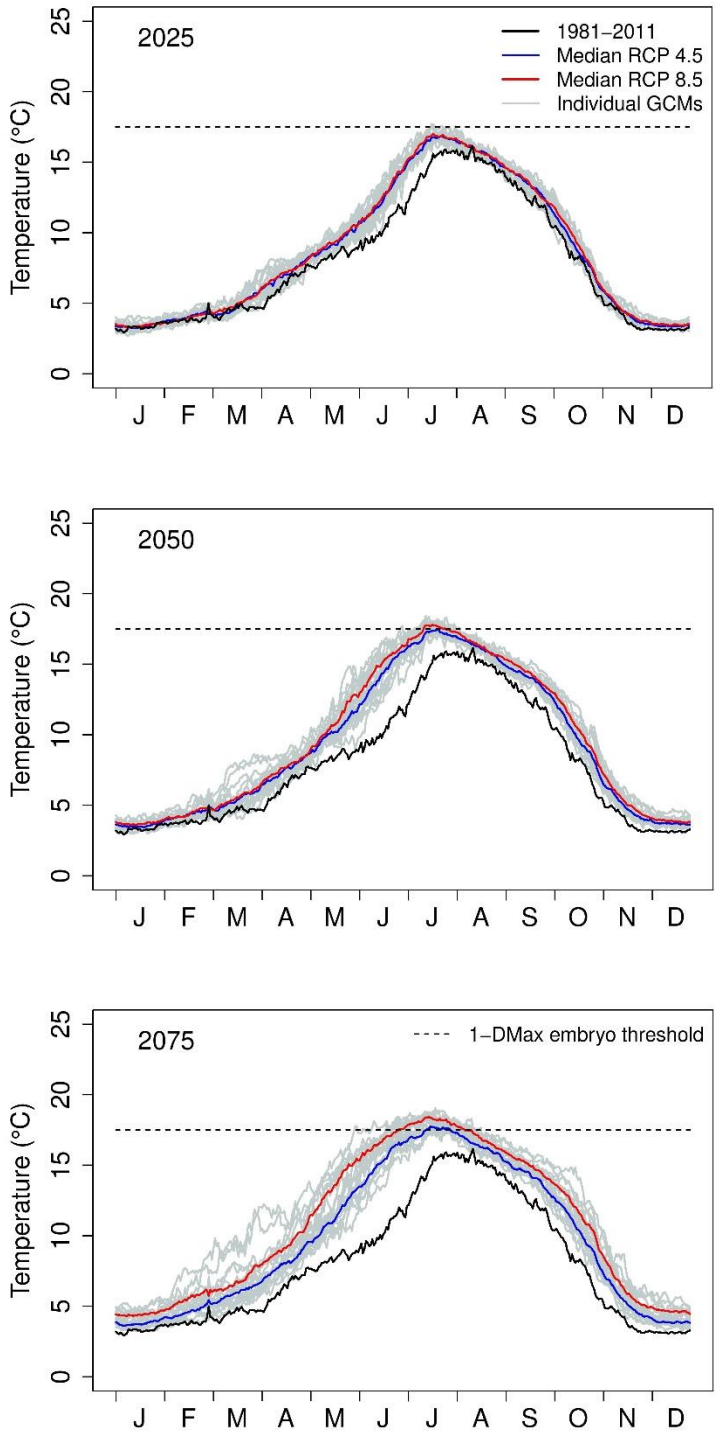

Figure 8. Monthly median stream temperature over three 30-year climate normal centered on the years 2025, 2050, and 2075 at the Ecology gauge. Median hindcast values (30-year climate normal centered on the year 1996) are represented by the black line. The median RCP 4.5 values are represented by the blue line. The median RCP 8.5 values are represented by the red line. The individual GCMs are represented by the gray lines. The horizontal dashed line represents the 1-DMax for salmon embryo mortality.

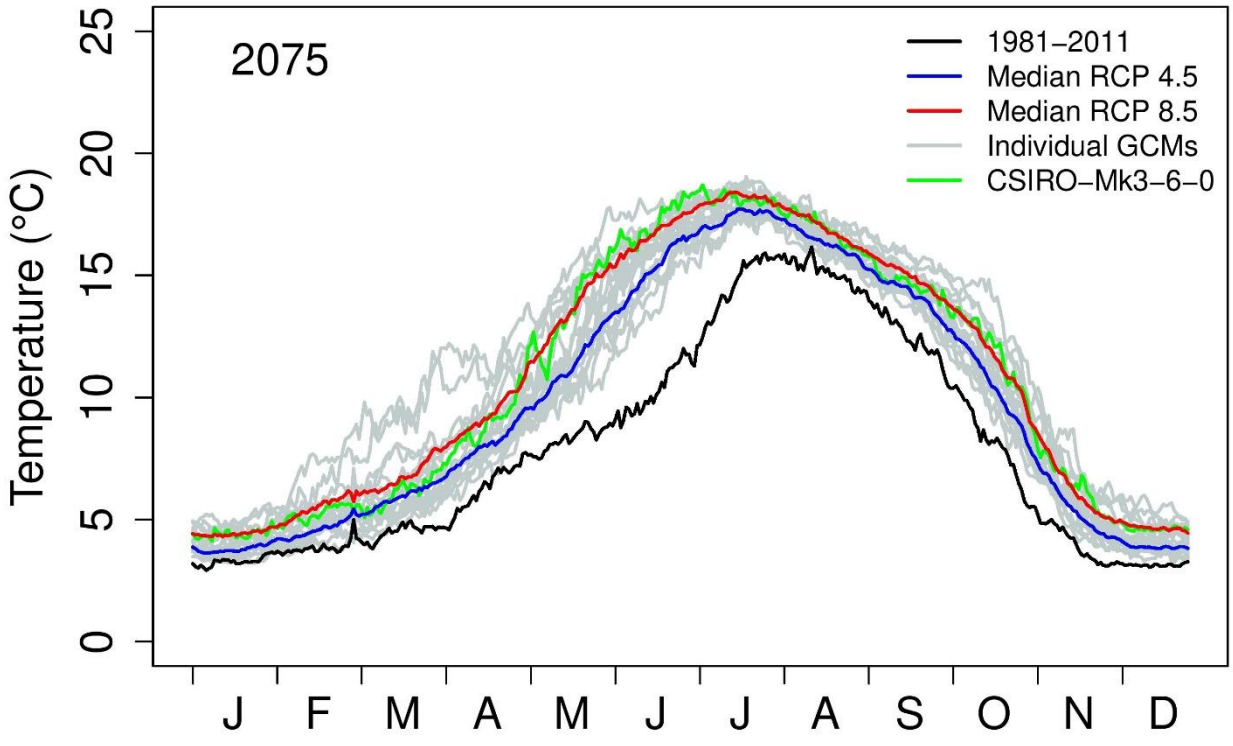

Figure 9. Verification that the CSIRO-Mk3-6-0 GCM (green line) is representative of the median of the 10 RCP 8.5 GCMs (red line). The blue line is the median of the RCP 4.5 GCMs, the black line represents the hindcast, and the grey lines represent individual GCMs.

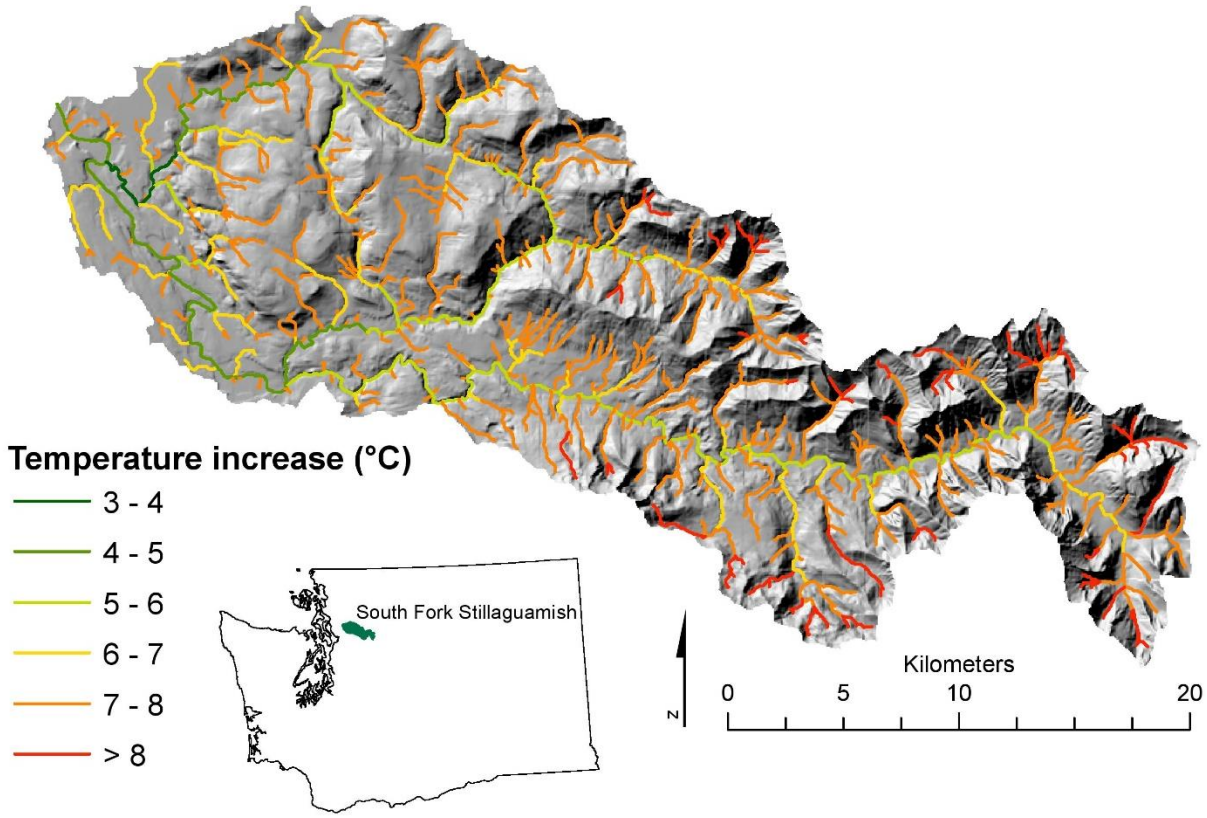

Figure 10. Modeled average July stream temperature increase at every stream segment in the South Fork Stillaguamish River basin between the hindcast and the 2075 climate normal under CSIRO-Mk3-6-0 GCM and RCP 8.5.

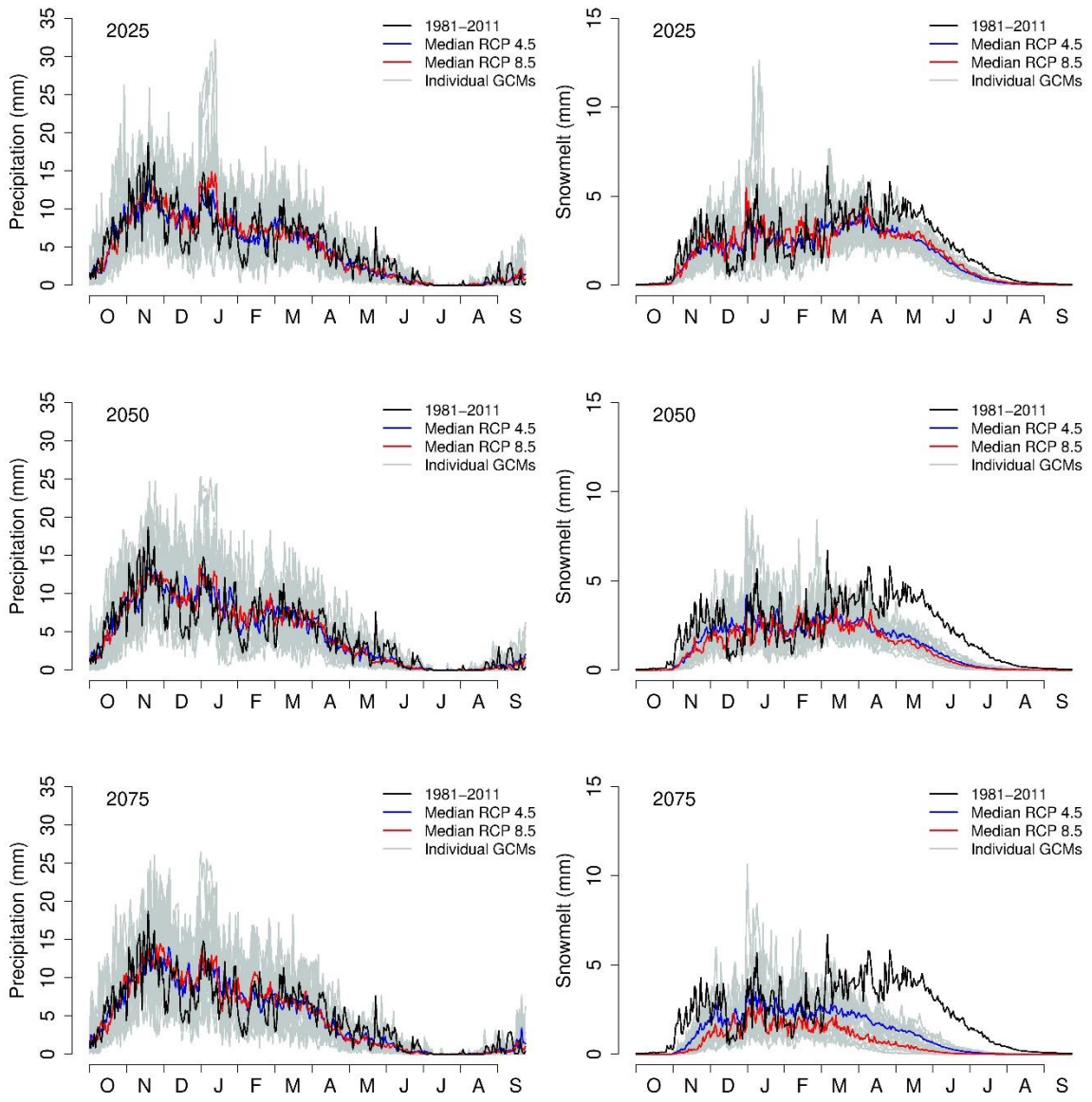

Figure 11. Modeled precipitation and snowmelt over three 30-year climate normal centered on the years 2025, 2050, and 2075. Median hindcast values (30-year climate normal centered on the year 1996) are represented by the black line. The median RCP 4.5 values are represented by the blue line. The median RCP 8.5 values are represented by the red line. The individual GCMs are represented by the gray lines.

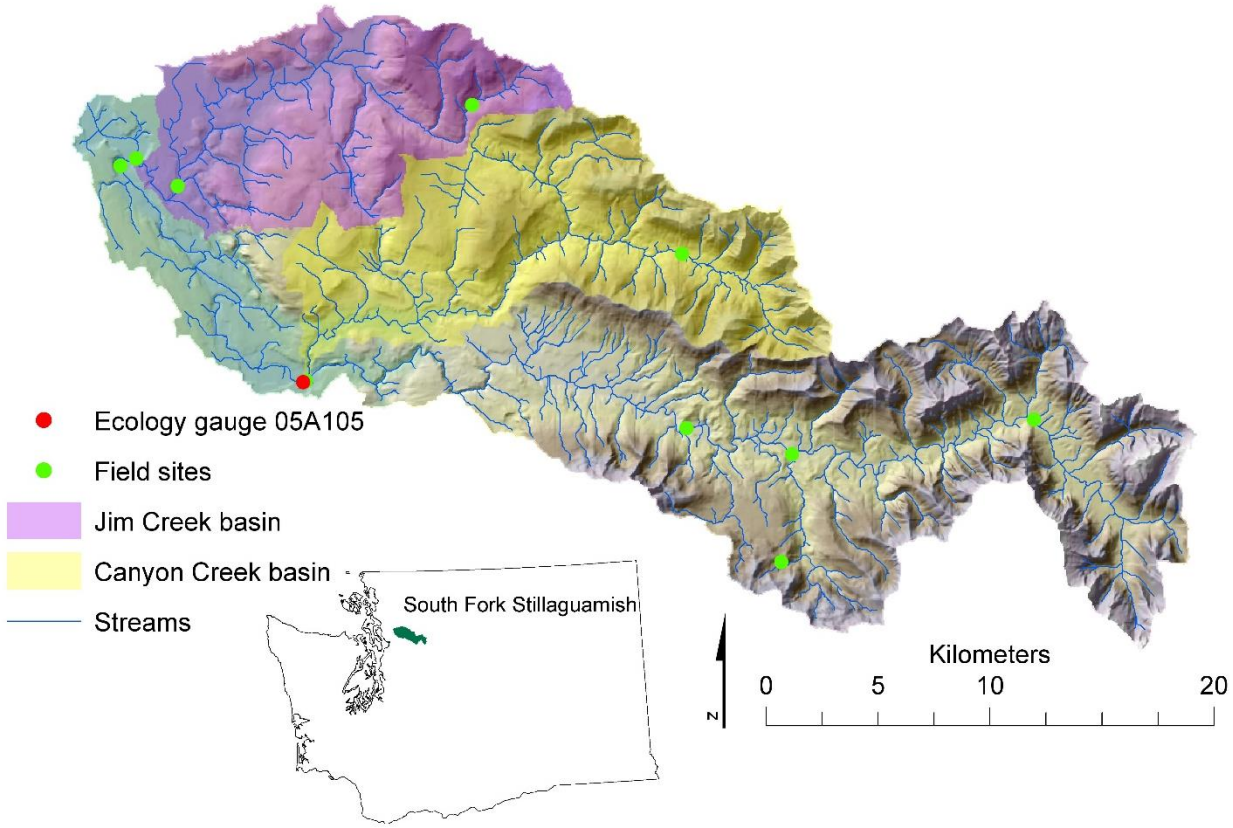

Figure 12. Sub-basins Jim Creek and Canyon Creek within the South Fork Stillaguamish River basin.

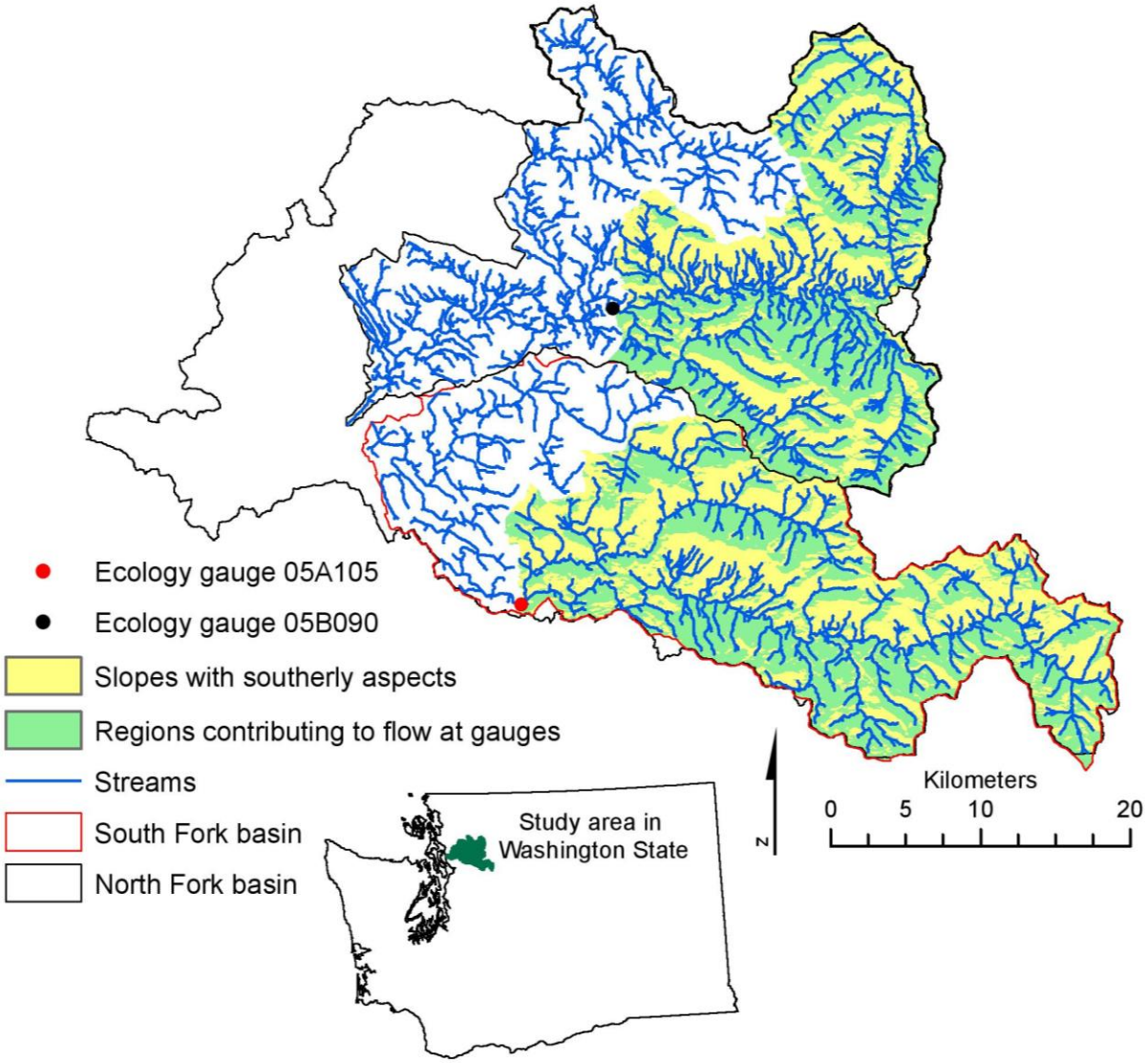

Figure 13. Regions of the Stillaguamish River basin with streams that have a southerly aspect.